

hep-ph/9602280
 Saclay-SPhT-T96/10

UCLA/96/TEP/5
 SLAC-PUB-7111

PROGRESS IN ONE-LOOP QCD COMPUTATIONS¹

Zvi Bern

Department of Physics, UCLA, Los Angeles, CA 90095

Lance Dixon

Stanford Linear Accelerator Center, Stanford University,
 Stanford, CA 94309

David A. Kosower

Service de Physique Théorique, Centre d'Etudes de Saclay,
 F-91191 Gif-sur-Yvette cedex, France

KEY WORDS: perturbative QCD, strings, unitarity, factorization

Contents

1	INTRODUCTION	2
1.1	<i>Importance of Diagrammatic Calculations</i>	2
1.2	<i>Difficulty of Brute-Force Calculations</i>	6
1.3	<i>Non-traditional Approaches</i>	8
2	PRIMITIVE AMPLITUDES	8
2.1	<i>Color Decomposition</i>	9
2.2	<i>Spinor Helicity Formalism</i>	12
2.3	<i>Parity and Charge Conjugation</i>	13
2.4	<i>Supersymmetry Identities</i>	14
3	STRING-INSPIRED METHODS	16
3.1	<i>String Organization</i>	16
3.2	<i>Supersymmetric Decomposition</i>	19

¹To appear in Annual Reviews of Nuclear and Particle Science (1996).

4	UNITARITY	21
4.1	<i>Cutkosky Rules</i>	22
4.2	<i>Cut Constructibility</i>	23
4.3	<i>Supersymmetric Examples</i>	26
4.4	<i>Non-supersymmetric Example</i>	30
5	FACTORIZATION	32
5.1	<i>General Framework</i>	33
5.2	<i>Examples</i>	36
6	CONCLUSIONS AND OUTLOOK	37

Abstract

We review progress in calculating one-loop scattering amplitudes required for next-to-leading-order corrections to QCD processes. The underlying technical developments include the spinor helicity formalism, color decompositions, supersymmetry, string theory, factorization and unitarity. We provide explicit examples illustrating these techniques.

1 INTRODUCTION

1.1 Importance of Diagrammatic Calculations

Gauge theories form the backbone of the Standard Model. The weak-coupling perturbative expansion of gauge theory scattering amplitudes, carried out by means of Feynman diagrams, has led to theoretical predictions in remarkable agreement with high-energy collider data [1]. This high-precision agreement places strong bounds on new physics. In the strong-interaction sector of the Standard Model — described by quantum chromodynamics — the precision is not as great as in the electroweak sector. QCD is asymptotically free, so the strong coupling constant α_s becomes weak at large momentum transfers, justifying a perturbative expansion [2]. Physical quantities do depend on nonperturbative, long-distance QCD, in the form of quantities such as parton distribution and fragmentation functions, as well as on the physics of hadronization. In many processes at modern colliders, however, the dominant theoretical uncertainties are due to an incomplete knowledge

of the perturbation series, rather than to our relative ignorance of non-perturbative aspects of scattering processes. The situation is exacerbated by the slow approach to asymptopia (α_s is of order 0.1 at the 100 GeV scale), and by the presence of large logarithms of ratios of scales.

The leading-order (LO) term in the α_s expansion of a QCD cross-section comes simply from squaring a tree-level scattering amplitude. Efficient techniques for computing QCD tree amplitudes have been available for some time now [3], and the results have provided a basic theoretical description of QCD processes and thereby estimates of QCD backgrounds to new physics searches. Unfortunately, higher order corrections, especially those enhanced by logarithms, can be sizeable. The ultraviolet logarithms manifest themselves in the residual renormalization-scale dependence of a finite-order prediction. The renormalization scale μ_R is introduced in order to define the coupling constant; renormalization group invariance requires any physical quantity to be independent of it. However, when a perturbative expansion is truncated at a finite order, residual μ_R -dependence appears, because the cancellation takes place across different orders in α_s . Calculations at next-to-leading order (NLO) in α_s significantly reduce the dependence on μ_R as compared to leading order. As an example, fig. 1 shows the comparison of the LO and NLO theoretical predictions to the experimental measurement of a point in the single-jet inclusive distribution. Note the good agreement between NLO theory and experiment and the significant reduction of theoretical uncertainties, compared to the LO calculation.

Infrared logarithms arise because jet processes involve more than one scale, at the very least a scale characterizing the jet size in addition to the hard scale of the short-distance scattering, and because of the infrared divergences of perturbative QCD. These divergences transform the perturbation expansion for such quantities from one in α_s alone to one in $\alpha_s \log^2 y_{\text{IR}}$ and $\alpha_s \log y_{\text{IR}}$ in addition to α_s , where y_{IR} is a jet ‘resolution’ parameter. All three must be small for the perturbation expansion to be reliable; but the first two cannot be calculated in an LO calculation. Only in an NLO calculation are the corresponding terms determined quantitatively, and only at this order can one establish the reliability of the perturbative calculation.

Beyond the logarithmically-enhanced corrections, the $\mathcal{O}(\alpha_s)$ corrections to most jet observables are larger than non-perturbative power corrections and corrections due to quark masses, and are thus the most important ones to calculate in order to refine the precision of theoretical predictions.

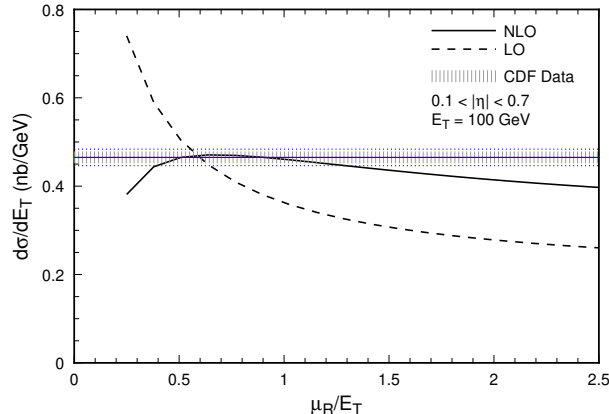


Figure 1: The inclusive cross section for single-jet production in $p\bar{p}$ collisions at $\sqrt{s} = 1.8$ TeV and jet transverse energy $E_T = 100$ GeV (using MRSD₀ structure functions [4]), showing the sensitivity of the LO result to the choice of renormalization scale, μ_R , and the reduced sensitivity at NLO. The CDF data shown is extracted from ref. [5]; the band shows statistical errors only.

Despite the need for higher-order QCD computations, at present no quantities have been computed beyond next-to-next-to-leading order (NNLO), and the only quantities that have been computed fully at NNLO are totally inclusive quantities such as the total cross-section for e^+e^- annihilation into hadrons, and the QCD corrections to various sum rules in deeply inelastic scattering [6, 7]. At NLO, there are many complete calculations (in the form of computer programs producing numerical results) for a variety of processes, but at present results are still limited to where the basic process has four external legs (counting electroweak vector bosons rather than their decay products as external legs). The following are examples of calculations which are relevant for current experiments but have not yet been performed or assembled:

1. NLO corrections to three-jet production at hadron colliders. These contributions would allow a measurement of α_s (via the three-jet to two-jet ratio) at the highest experimentally available momentum transfers, as well as next-to-leading-order studies of jet structure.
2. NLO corrections to W + multi-jet production at hadron collid-

ers. These processes form a background to the t quark signal at Fermilab.

3. NLO corrections to $e^+e^- \rightarrow 4$ jets. At the Z resonance, this is the lowest-order process in which the quark and gluon color charges can be measured independently. It will also be useful for ruling out the presence of light colored fermions (or scalars). At LEP2 it is a background to threshold production of W pairs, when both W 's decay hadronically.
4. NNLO corrections to $e^+e^- \rightarrow 3$ jets. These corrections are the dominant uncertainty in a precision extraction of α_s from hadronic event shapes at the Z [8].

In any of these processes, deviations of experimental results from the theoretical predictions could indicate new physics.

Why do these higher-order QCD corrections remain uncalculated? NLO corrections can be divided into real and virtual parts. (See fig. 2.) Real corrections arise from the emission of one additional parton into the final state, and are straightforward to compute from tree amplitudes with one more leg than the LO tree amplitude. Virtual corrections arise from the interference of the LO tree amplitude with a one-loop amplitude. Each contribution is infrared divergent, but the divergences cancel in the sum, after integrating the real contribution over “unobserved” partons in the final state [9], and factorizing initial state singularities into the definition of parton distributions in an incoming hadron [10]. The remaining finite integrations are typically performed with a numerical program [11].

While the numerical evaluation of NLO corrections can be non-trivial, the major analytical bottleneck is simply the availability of one-loop amplitudes, which enter into the virtual corrections. In particular, one-loop amplitudes with more than four external legs (and all quarks massless), which are required for the higher-order corrections listed above, have only recently become available, thanks to the development of new calculational techniques. The purpose of this review is to provide an introduction to some of these techniques, together with worked-out examples.

Our emphasis will be on obtaining compact analytic results. In general, it is preferable to have such results for matrix elements, even though they are ultimately inserted into numerical programs for computing cross-sections. Without compact results, numerical instabilities can arise from the vanishing of spurious denominators in the expression.

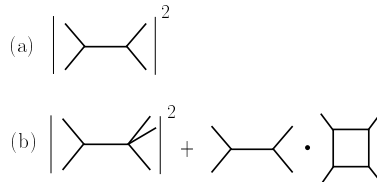


Figure 2: In (a) the parton subprocesses required for the LO contribution to two-jet production at hadron colliders are shown schematically. In (b) the corresponding real and virtual NLO contributions are shown.

With analytic forms it is also easier to compare independent calculations, to understand better how to organize calculations, and even to obtain results for an arbitrary number of external legs [12, 13, 14, 15].

1.2 Difficulty of Brute-Force Calculations

Gauge theories have an elegant construction based on the principle of local gauge invariance. The QCD Lagrangian for massless quarks q is

$$\mathcal{L}_{QCD} = -\frac{1}{4}\text{Tr}(F_{\mu\nu}^2) - i\bar{q}\not{D}q, \quad (1)$$

where the covariant derivative $D_\mu = \partial_\mu - igA_\mu/\sqrt{2}$ and field strength $F_{\mu\nu} = i\sqrt{2}[D_\mu, D_\nu]/g$ are given in terms of the matrix-valued gauge connection $A_\mu = A_\mu^a T^a$.² Since \mathcal{L}_{QCD} depends on a single coupling constant g , all the interactions are dictated by gauge symmetry. Unfortunately, the Feynman diagram expansion does not respect this invariance, because the quantization procedure fixes the gauge symmetry. Individual diagrams are not gauge invariant, and are often more complicated than the final sum over diagrams. The non-abelian gluon self-interactions coming from the cubic and quartic terms in eq. (1) have a complicated index structure and momentum-dependence. So while it is straightforward in principle to compute both tree and loop amplitudes by drawing all Feynman diagrams and evaluating them, in practice this method becomes extremely inefficient and cumbersome as the number of external legs grows. For five or more external legs there are a large

² The normalization $\text{Tr}(T^a T^b) = \delta^{ab}$ of the fundamental-representation generators T^a accounts for the $\sqrt{2}$'s here; it serves to eliminate the $\sqrt{2}$'s from the partial amplitudes defined below.

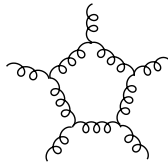


Figure 3: The five-gluon pentagon diagram.

number of kinematic variables, which allow the construction of complicated expressions. Indeed, intermediate expressions tend to be vastly more complicated than the final results, when the latter are represented in an appropriate way.

As an example consider the five-gluon pentagon diagram, depicted in fig. 3, which would be encountered in a brute-force computation of NLO corrections to three-jet production at a hadron collider. Each of the five non-abelian three-point vertices in the diagram is given by

$$V_{\mu\nu\rho}^{abc}(k, p, q) = f^{abc} \left(\eta_{\nu\rho}(p - q)_\mu + \eta_{\rho\mu}(q - k)_\nu + \eta_{\mu\nu}(k - p)_\rho \right), \quad (2)$$

where f^{abc} are the $SU(3)$ structure constants, k , p and q the momenta, and $\eta_{\mu\nu}$ the Minkowski metric. As the non-abelian vertex has six terms, a rough estimate of the number of terms is about 6^5 . Each term is associated with a loop integral which evaluates to an expression on the order of a page in length. This means that one is faced with about 10^4 pages of algebra for this single diagram. As bad as this brute-force approach might seem, the situation is actually worse, because of the structure of the results. After evaluating the integrals and summing over a few hundred more diagrams one obtains expressions of the form $\sum_i \frac{N_i}{D_i}$, where the factors N_i are polynomials in the gluon polarization vectors and external momenta, and the D_i (polynomials in the external invariants) are produced when the loop integrals are reduced to a standard set of functions. In general the D_i contain spurious kinematic singularities which cancel only after combining many terms over a common denominator; this causes an explosion of terms in the numerator.

In contrast to the complexity of intermediate expressions, the final results can be strikingly simple. For example, the five gluon amplitudes which we shall describe in section 3.2 are remarkably compact.

1.3 *Non-traditional Approaches*

Substantial progress has been made in the past decade in improving the calculation of tree-level amplitudes. Four ideas which have played an important role are the spinor helicity method for gluon polarization vectors [16], the color decomposition [17], supersymmetry identities [18, 19], and the Berends and Giele recurrence relations [20]. Although these ideas form a basis for the one-loop techniques described here, they have been extensively reviewed in ref. [3, 21], and we permit ourselves only a brief review below.

As illustrated by the pentagon example above, one-loop computations are significantly more complicated than tree computations, so further techniques are useful for preventing an explosion in algebra. The additional ideas which we shall discuss in this review involve string theory, supersymmetry, unitarity, and factorization. String theory, for example, suggests better gauge choices, a supersymmetric decomposition of amplitudes, and an improved disentanglement of color and kinematics. Approaches based on unitarity and factorization make use of the analytic properties of amplitudes to build further amplitudes using known ones. Since these approaches use gauge-invariant quantities as the basic building blocks of new amplitudes they tend to be extremely efficient. Although we shall not discuss recursion relations here, Mahlon has made considerable progress in applying these to one-loop amplitudes [13]. For simplicity, we demonstrate the methods for amplitudes where all external particles are gluons, even though most of the techniques (or analogs of them) can be applied to amplitudes with external fermions as well.

To date, these techniques have allowed for the computation of all one-loop five-parton helicity amplitudes [22, 23, 24], as well several infinite sequences of one-loop amplitudes [12, 13, 14, 15]. The five-parton amplitudes are currently being incorporated into numerical programs for NLO three-jet production at hadron colliders, the first item on the list in Section 1.1 [25]. Thus the analytical bottleneck to NLO corrections is yielding to the new techniques described in this review.

2 PRIMITIVE AMPLITUDES

In this section, we briefly review the use of color and helicity information to decompose amplitudes into ‘primitive amplitudes’. These building blocks have a much simpler analytic structure than the full amplitudes, a fact which will be exploited in subsequent sections. We also review the application of supersymmetric Ward identities to QCD.

2.1 Color Decomposition

Color decompositions have a long history, dating back to Chan-Paton factors in early formulations of string theory [17]. They are also related to the “double-line” formalism introduced by ‘t Hooft in the large- N_c (number of colors) approach to QCD [26], although here we will not make any large- N_c or “leading-color” approximations. The basic idea is to use group theory to break up an amplitude into gauge-invariant pieces which are composed of Feynman diagrams with a fixed cyclic ordering of external legs. These pieces are simpler because poles and cuts can only appear in kinematic invariants made out of cyclicly adjacent sums of momenta, of the form $(k_i + k_{i+1} + \dots + k_j)^2$. At the four-point level this is not so important, because only one of the three Mandelstam variables s, t, u is thereby excluded; but as the number of external legs grows, the total number of invariants grows much faster than the number of cyclicly adjacent ones. The following brief review focuses on results needed later, rather than derivations. A more complete discussion can be found in refs. [17, 3, 27, 14, 24, 21].

We first generalize the gauge group of QCD to $SU(N_c)$, with the quarks transforming in the fundamental representation. The simplest way to implement the color decomposition in field theory is by rewriting the group structure constants appearing in Feynman diagrams in terms of fundamental representation matrices

$$f^{abc} = -\frac{i}{\sqrt{2}} \left(\text{Tr}(T^a T^b T^c) - \text{Tr}(T^b T^a T^c) \right). \quad (3)$$

After making this substitution in a generic Feynman diagram we obtain a large number of traces, many sharing T^a ’s with contracted indices, of the form $\text{Tr}(\dots T^a \dots) \text{Tr}(\dots T^a \dots) \dots \text{Tr}(\dots)$. If external quarks are present, then in addition to the traces there will be some strings of T^a ’s terminated by fundamental indices. To reduce the number of traces and strings to a minimum, we rearrange the contracted T^a ’s, using

$$(T^a)_{i_1}^{\bar{j}_1} (T^a)_{i_2}^{\bar{j}_2} = \delta_{i_1}^{\bar{j}_2} \delta_{i_2}^{\bar{j}_1} - \frac{1}{N_c} \delta_{i_1}^{\bar{j}_1} \delta_{i_2}^{\bar{j}_2}, \quad (4)$$

where the sum over a is implicit. (If all lines are in the adjoint representation the second term drops out by a $U(1)$ decoupling identity [3, 17], which follows from the lack of a ‘photon’ self-coupling.) A *partial amplitude* is the coefficient of a given color trace in the resulting color decomposition of the amplitude.

For example, in the n -gluon tree amplitude, application of eq. (4) reduces all color factors to single traces. Thus its decomposition is

$$\mathcal{A}_n^{\text{tree}} = g^{n-2} \sum_{\sigma \in S_n/Z_n} \text{Tr}(\sigma(1) \dots \sigma(n)) A_n^{\text{tree}}(\sigma(1), \dots, \sigma(n)), \quad (5)$$

where A_n^{tree} are the partial amplitudes, $\text{Tr}(1 \dots n) \equiv \text{Tr}(T^{a_1} \dots T^{a_n})$, with a_i the color index of the i -th external gluon, and S_n/Z_n is the set of non-cyclic permutations of $\{1, 2, \dots, n\}$, corresponding to the set of inequivalent traces. The labels on the gluon momenta k_i and polarization vectors ε_i , implicit in eq. (5), are also to be permuted by σ . In the next subsection we will go over to a helicity basis, and the label i will be replaced by i^{λ_i} , with λ_i the (outgoing) gluon helicity. Similarly, tree amplitudes with a pair of external quarks can be reduced to a sum over single strings of matrices, $(T^{a_3} \dots T^{a_n})_{i_2^{\bar{j}_1}}$, and so on. For a proof that individual partial amplitudes are gauge invariant, see ref. [3].

At one loop, additional color structures are possible; in the n -gluon amplitude double traces appear as well as single traces. For example, the color decomposition of the one-loop five-gluon amplitude is

$$\begin{aligned} \mathcal{A}_5^{1\text{-loop}} = & g^5 \mu_R^{2\epsilon} \left[\sum_{\sigma \in S_5/Z_5} N_c \text{Tr}(\sigma(1) \dots \sigma(5)) A_{5;1}(\sigma(1), \dots, \sigma(5)) \right. \\ & \left. + \sum_{\sigma \in S_5/(S_2 \times S_3)} \text{Tr}(\sigma(1)\sigma(2)) \text{Tr}(\sigma(3)\sigma(4)\sigma(5)) A_{5;3}(\sigma(1), \sigma(2); \sigma(3), \sigma(4), \sigma(5)) \right]; \end{aligned} \quad (6)$$

as in eq. (5) the permutation sums are over all inequivalent traces. For gauge group $U(N_c)$, the partial amplitudes $A_{5;2}$ multiplying traces of the form $\text{Tr}(1)\text{Tr}(2345)$ would also have to be included, but for $SU(N_c)$ the trace of a single generator vanishes. The decomposition of the n -gluon amplitude into single-trace ($A_{n;1}$) and double-trace ($A_{n;j>2}$) components is entirely analogous. Were one to consider the large- N_c limit, the single-trace terms would give rise to the leading contributions, and we will refer to the corresponding partial amplitudes as leading-color partial amplitudes; the double-trace terms have subleading-color partial amplitudes as coefficients.

The rules for constructing leading-color partial amplitudes such as A_n^{tree} and $A_{n;1}$ are *color-ordered* Feynman rules, which are depicted in fig. 4 for the standard Lorentz-Feynman gauge. These rules are obtained from ordinary Feynman rules by restricting attention to a given ordering of color matrices. Applying eq. (3) to eq. (2) and extracting the coefficient of $\text{Tr}(T^a T^b T^c)$ gives the color-ordered three-vertex

$$\begin{aligned}
\text{Diagram 1: } & \text{Three-gluon vertex with incoming gluons } (q, \rho), (p, \nu) \text{ and outgoing gluon } (k, \mu) \\
& = \frac{i}{\sqrt{2}} (\eta_{\nu\rho}(p-q)_\mu + \eta_{\rho\mu}(q-k)_\nu + \eta_{\mu\nu}(k-p)_\rho) \\
\text{Diagram 2: } & \text{Four-gluon vertex with incoming gluons } (\mu, \lambda), (\nu, \rho) \text{ and outgoing gluons } (\nu, \mu), (\rho, \lambda) \\
& = i\eta_{\mu\rho}\eta_{\nu\lambda} - \frac{i}{2}(\eta_{\mu\nu}\eta_{\rho\lambda} + \eta_{\mu\lambda}\eta_{\nu\rho}) \\
\text{Diagram 3: } & \text{Feynman rule for a gluon-fermion vertex with incoming fermion and outgoing gluon } (\mu) \\
& = \frac{i}{\sqrt{2}}\gamma_\mu \\
\text{Diagram 4: } & \text{Feynman rule for a gluon-fermion vertex with incoming gluon } (\mu) \text{ and outgoing fermion } (\nu) \\
& = -i\frac{\eta_{\mu\nu}}{p^2} \\
\text{Diagram 5: } & \text{Feynman rule for a fermion-fermion vertex with incoming fermion and outgoing fermion } (\mu) \\
& = -\frac{i}{\sqrt{2}}\gamma_\mu \\
\text{Diagram 6: } & \text{Feynman rule for a fermion-fermion vertex with incoming fermion and outgoing fermion } (\mu) \\
& = \frac{i}{\not{p}}
\end{aligned}$$

Figure 4: Color-ordered Feynman rules in Lorentz-Feynman gauge. Curly lines represent gluons and lines with arrows fermions.

in fig. 4; and similarly for the color-ordered four-vertex, the coefficient of $\text{Tr}(T^a T^b T^c T^d)$. The only diagrams to be computed are those that can be drawn in a planar fashion with the external legs following the ordering of the color trace under consideration.

The immediate advantage of rewriting Feynman rules in this way is that fewer diagrams contribute to a given partial amplitude, and its analytic structure is simpler. As a simple example, with conventional Feynman diagrams one would have a total of four conventional Feynman diagrams, depicted in fig. 5 for the four-point tree amplitude. With color-ordered Feynman rules one would compute the partial amplitude $A_4(1, 2, 3, 4)$ associated with the color trace $\text{Tr}(T^{a_1} T^{a_2} T^{a_3} T^{a_4})$, omitting diagram 5c since the ordering of the legs do not follow the ordering of the color trace. Thus $A_4(1, 2, 3, 4)$ has no pole in $(k_1 + k_3)^2$. The other partial amplitudes can be obtained by permuting the arguments of $A_4(1, 2, 3, 4)$. For the five-gluon amplitude, there are 10 color-ordered diagrams as opposed to 40 total. Obviously the simplifications obtained using partial amplitudes increase rapidly with the number of external legs.

At one loop, one also has to compute subleading-color partial amplitudes, such as the double-trace coefficients $A_{5;3}$ in eq. (6), which cannot be obtained directly from color-ordered rules. Fortunately there exist general formulas relating such quantities to permutation sums of color-ordered objects [27, 14, 24]. For example, the gluon-loop contribution

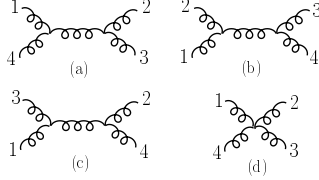


Figure 5: The four-point Feynman diagrams. Color-ordered Feynman rules do not include diagram (c) for $A_4(1, 2, 3, 4)$.

to the four-gluon amplitude can be found from the relation

$$A_{4;3}(1, 2; 3, 4) = A_{4;1}(1, 2, 3, 4) + A_{4;1}(1, 3, 2, 4) + A_{4;1}(2, 1, 3, 4) \\ + A_{4;1}(2, 3, 1, 4) + A_{4;1}(3, 1, 2, 4) + A_{4;1}(3, 2, 1, 4). \quad (7)$$

Such formulæ can be derived from string theory [28, 14], although the most straightforward way to prove them is using color flow diagrams in field theory [24]. To understand formula (7) heuristically, it is useful to focus on the box diagram. Using ordinary Feynman rules and expanding out the structure constants using eqs. (3) and (4) it is straightforward to check that the box diagrams contribute to $A_{4;1}$ and $A_{4;3}$ in such a way that eq. (7) is satisfied. Roughly speaking, gauge invariance then requires the remaining diagrams to tag along properly with the box diagram.

Thus we can restrict our discussion henceforth to amplitudes with a fixed ordering of external legs, which we call *primitive amplitudes*. In the n -gluon cases discussed above, the set of primitive amplitudes coincides with the leading-color partial amplitudes A_n^{tree} and $A_{n;1}$, but this is not always the case. For example, one-loop amplitudes with external fermions have leading-color (as well as subleading-color) partial amplitudes that are sums of several primitive amplitudes [24].

2.2 Spinor Helicity Formalism

In explicit calculations, it is very convenient to adopt a helicity (circular polarization) basis for external gluons. The spinor helicity formalism [16] expresses the positive- and negative-helicity polarization vectors in terms of massless Weyl spinors $|k^\pm\rangle$,

$$\varepsilon_\mu^+(k; q) = \frac{\langle q^- | \gamma_\mu | k^- \rangle}{\sqrt{2} \langle q k \rangle}, \quad \varepsilon_\mu^-(k; q) = \frac{\langle q^+ | \gamma_\mu | k^+ \rangle}{\sqrt{2} [k q]}, \quad (8)$$

where q is an arbitrary null ‘reference’ momentum which drops out of the final gauge-invariant amplitudes. (Changing q is equivalent to performing a gauge transformation on the external legs.) We use the compact notation

$$\langle k_i^- | k_j^+ \rangle \equiv \langle ij \rangle, \quad \langle k_i^+ | k_j^- \rangle \equiv [ij]. \quad (9)$$

These spinor products are crossing-symmetric, antisymmetric in their arguments, and satisfy

$$\langle ij \rangle [j i] = 2k_i \cdot k_j \equiv s_{ij}. \quad (10)$$

Helicity amplitudes can be given a manifestly crossing symmetric representation, with the convention that a helicity label corresponds to an outgoing particle; the helicity of an incoming particle is reversed. As we shall discuss in Section 5, in the collinear limit where k_i and k_j become parallel, helicity amplitudes have a square-root singular behavior, $\sim \frac{1}{\sqrt{s_{ij}}} \sim \frac{1}{\langle ij \rangle} \sim \frac{1}{[ij]}$, whose magnitude and phase are captured concisely by the spinor products. This helps explain why spinor products provide an extremely compact representation of amplitudes.

In performing calculations, the Schouten identity is useful,

$$\langle ij \rangle \langle kl \rangle = \langle il \rangle \langle kj \rangle + \langle ik \rangle \langle jl \rangle. \quad (11)$$

A more complete discussion, including further identities and numerical representations of the spinor products, can be found in refs. [16, 3, 21].

To maximize the benefit of the spinor helicity formalism for loop amplitudes we must choose a compatible regularization scheme. In conventional dimensional regularization [29], the polarization vectors are $(4 - 2\epsilon)$ -dimensional; this is incompatible with the spinor helicity method, which assumes four-dimensional polarizations. To avoid this problem, we modify the regularization scheme so all helicity states are four-dimensional and only the loop momentum is continued to $(4 - 2\epsilon)$ dimensions. This is the four-dimensional-helicity (FDH) scheme [28], which has been shown to be equivalent [30] to an appropriate helicity formulation of Siegel’s dimensional-reduction scheme [31] at one-loop. The conversion between schemes has been given in ref. [30], so there is no loss of generality in choosing the FDH scheme.

2.3 Parity and Charge Conjugation

The reader might worry that the color and helicity decompositions will lead to a huge proliferation in the number of primitive or partial amplitudes that have to be computed. In fact, this does not happen, thanks

to the group theory relations mentioned above, plus the discrete symmetries of parity and charge conjugation. Parity simultaneously reverses all helicities in an amplitude; eq. (8) shows that it is implemented by the exchange $\langle i j \rangle \leftrightarrow [j i]$. Charge conjugation is related to the anti-symmetry of the color-ordered rules; for pure-gluon partial amplitudes it takes the form of a reflection identity,

$$A_n^{\text{tree}}(1, 2, \dots, n) = (-1)^n A_n^{\text{tree}}(n, \dots, 2, 1). \quad (12)$$

For amplitudes with external quarks, it allows one to exchange a quark and anti-quark, or equivalently to flip the helicity on a quark line.

As an example, with the use of parity and cyclic (Z_5) symmetry, we can reduce the five-gluon amplitude at tree level to a combination of just four independent partial amplitudes:

$$\begin{aligned} A_5^{\text{tree}}(1^+, 2^+, 3^+, 4^+, 5^+), & \quad A_5^{\text{tree}}(1^-, 2^+, 3^+, 4^+, 5^+), \\ A_5^{\text{tree}}(1^-, 2^-, 3^+, 4^+, 5^+), & \quad A_5^{\text{tree}}(1^-, 2^+, 3^-, 4^+, 5^+). \end{aligned} \quad (13)$$

Furthermore, the first two partial amplitudes here vanish (see below), and there is a group theory ($U(1)$ decoupling) relation between the last two [3, 21], so there is only one independent nonvanishing object to calculate. At one loop there are four independent objects — eq. (13) with A_5^{tree} replaced by $A_{5;1}$ — but only the last two contribute to the NLO cross-section, due to the tree-level vanishings. The explicit expression for $A_{5;1}(1^-, 2^-, 3^+, 4^+, 5^+)$ is given in section 3.2.

2.4 Supersymmetry Identities

What does supersymmetry have to do with a non-supersymmetric theory such as QCD? The answer is that tree-level QCD is “effectively” supersymmetric [19]. Consider an n -gluon tree amplitude. It has no loops in it, so it has no fermion loops in it. The fermions in the theory might as well be in the adjoint representation, that is, the theory might as well be a super Yang-Mills theory. Pure-gluon tree amplitudes in QCD are indeed identical to those in the supersymmetric theory, and are thus related by supersymmetry to amplitudes with fermions (the gluinos). It is however more useful to think of such relations as connecting *partial* amplitudes. These relations are the so-called supersymmetric Ward identities (SWI) [18, 3, 21]. They connect pure-gluon partial amplitudes to partial amplitudes with a quark pair, because after the color information has been stripped off, the latter are identical to partial amplitudes with gluinos instead of quarks. Using the SWI saves computational labor [19].

The SWI relate amplitudes with all external gluons, g , to amplitudes where a pair of gluons is replaced by a pair of gluinos, Λ , or a pair of complex scalars, ϕ . Specifically, the SWI that we shall make use of in later sections are

$$\begin{aligned}
A_n^{\text{SUSY}}(g_1^\pm, g_2^+, \dots, g_n^+) &= 0, \\
A_n^{\text{SUSY}}(\Lambda_1^-, g_2^+, \dots, g_{n-1}^+, \Lambda_n^+) &= 0, \\
A_n^{\text{SUSY}}(\phi_1^-, g_2^+, \dots, g_{n-1}^+, \phi_n^+) &= 0, \\
A_n^{\text{SUSY}}(\Lambda_1^-, g_2^+, \dots, g_j^-, \dots, \Lambda_n^+) &= \frac{\langle j n \rangle}{\langle j 1 \rangle} A_n^{\text{SUSY}}(g_1^-, g_2^+, \dots, g_j^-, \dots, g_n^+), \\
A_n^{\text{SUSY}}(\phi_1^-, g_2^+, \dots, g_j^-, \dots, \phi_n^+) &= \frac{\langle j n \rangle^2}{\langle j 1 \rangle^2} A_n^{\text{SUSY}}(g_1^-, g_2^+, \dots, g_j^-, \dots, g_n^+),
\end{aligned} \tag{14}$$

where ‘...’ denotes positive-helicity gluons, and the helicity assignments on ϕ refer to particle or antiparticle assignments rather than genuine helicity. At tree level, these identities hold for all QCD partial amplitudes; for supersymmetric partial amplitudes, they hold to all orders in perturbation theory.

At one loop QCD “knows” that it is not supersymmetric, but one can still perform a supersymmetric decomposition of a QCD amplitude (see section 3.2), for which the supersymmetric components of the amplitude will obey eq. (14). One may also use the identities to find relations amongst non-supersymmetric contributions. For example, in $N = 1$ super-Yang-Mills, one can use the first of the identities in eq. (14) to deduce that fermion- and gluon-loop contributions are equal and opposite for n -gluon amplitudes with maximal helicity violation. By considering an $N = 2$ theory, with one gluon, two gluinos and one (complex) scalar, one deduces that all three types of loop contribution must be proportional to each other. We therefore obtain, for $SU(N_c)$ QCD with n_s massless complex scalars and n_f massless Dirac fermions,

$$A_{n;1}(g_1^\pm, g_2^+, \dots, g_n^+) = \left(1 + \frac{n_s}{N_c} - \frac{n_f}{N_c}\right) A_{n;1}^{\text{scalar}}(g_1^\pm, g_2^+, \dots, g_n^+), \tag{15}$$

where $A_{n;1}^{\text{scalar}}$ is the contribution of a single scalar and the factors of $1/N_c$ are the conversion factors between the adjoint and fundamental representation loops. (Note that adjoint representation complex scalars have two states, but we have chosen the normalization that scalars in the fundamental representation — $N_c \oplus \overline{N}_c$ — have four states, the same as for their would-be superpartner fermions.)

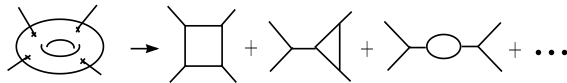


Figure 6: A single string diagram implicitly contains all field theory Feynman diagrams.

3 STRING-INSPIRED METHODS

String theory has provided a number of improvements in the calculation of one-loop amplitudes. Originally, we used it to derive a set of diagrammatic computational rules for calculating gluon amplitudes [28, 32]. Such rules were used in the first computation of the one-loop five-gluon amplitudes [22]. The same methods also work well for gravity calculations [33]. One of the authors has reviewed the string-based rules in ref. [34] and we shall not do so here. Other approaches to the string-based rules have been formulated [35, 36]. In particular, the first-quantized particle world-line has led to a rather efficient computation of the two-loop QED β -function [37] and of coefficients of high-dimension operators in effective actions.

3.1 String Organization

The basic motivation for the use of string theory follows from the compact representation it provides for amplitudes: at each loop order there is only a single closed string diagram. As depicted in fig. 6, the string theory diagram contains within it all the Feynman diagrams, including contributions of the entire tower of superheavy string excitations. The unwanted superheavy contributions are removed by taking the “low-energy limit” where all external momentum invariants are much less than the string tension. This limit picks out different regions of integration in the string diagram (see fig. 6), corresponding roughly to particle-like diagrams, but with different, string-based, rules [32].

Given knowledge of the string-based rules and organization, one may also formulate a conventional field-theory framework which mimics them [38] (at least for one-loop multiparton amplitudes), but which can be applied more broadly (for example, to amplitudes with external fermions). At one loop, key ingredients of this string-inspired framework are: use of a special gauge which is a hybrid of Gervais-Neveu gauge [39] and background-field gauge [40]; improved color decompositions; systematic organization of the algebra; and a second-order formalism for fermions

$$\begin{aligned}
& \text{Diagram 1: A horizontal wavy line with two external indices } \mu \text{ and } \nu. \quad = -i \frac{\eta_{\mu\nu}}{p^2} \\
& \text{Diagram 2: A wavy line with three external indices } \rho, q, \text{ and } k. \quad = i\sqrt{2}(\eta_{\mu\nu}k_\rho + \eta_{\nu\rho}p_\mu + \eta_{\rho\mu}q_\nu) \\
& \text{Diagram 3: A wavy line with four external indices } \mu, \nu, \lambda, \text{ and } \rho. \quad = i\eta_{\mu\rho}\eta_{\nu\lambda}
\end{aligned}$$

Figure 7: The color-ordered Gervais-Neveu gauge three- and four-point vertices.

[38, 41] which helps make supersymmetry relations manifest.

Gervais-Neveu gauge, originally derived from the low-energy limit of tree-level string amplitudes [39], has the following gauge-fixed action (ignoring ghosts):

$$S^{\text{GN}} = \int d^4x \left(-\frac{1}{4} \text{Tr}[F_{\mu\nu}^2] - \frac{1}{2} \text{Tr}[(\partial \cdot A - igA^2/\sqrt{2})^2] \right). \quad (16)$$

The color-ordered Feynman rules derived from this action are depicted in fig. 7; comparing them to the color-ordered vertices for the standard Lorentz-Feynman gauge (fig. 4), we see that the three-point and four-point vertices have, respectively, half and a third as many terms, showing why the Gervais-Neveu gauge is simpler for tree-level calculations.

Given this understanding of the string reorganization of tree amplitudes, one might guess that string theory would best be described by the Gervais-Neveu gauge at one loop as well. However, the gauge most closely resembling the string organization of one-loop amplitudes is a hybrid gauge involving both background-field and Gervais-Neveu gauges [38]. To quantize in a background-field gauge [40] one splits the gauge field into a classical background field and a fluctuating quantum field, $A_\mu = A_\mu^B + A_\mu^Q$, and imposes the gauge condition $D_\mu^B A_\mu^Q = 0$, where $D_\mu^B = \partial_\mu - \frac{i}{\sqrt{2}}gA_\mu^B$ is the background-field covariant derivative, with A_μ^B evaluated in the adjoint representation. The Feynman-gauge version of the gauge-fixed action is (again ignoring ghosts),

$$S^{\text{Bkgd}} = \int d^4x \left(-\frac{1}{4} \text{Tr}[F_{\mu\nu}^2] - \frac{1}{2} \text{Tr}[(\partial \cdot A^Q - ig[A_\mu^B, A_\mu^Q]/\sqrt{2})^2] \right). \quad (17)$$

The color-ordered background-field gauge vertices which arise from expanding eq. (17) are depicted in fig. 8. Here we show only the vertices

$$\begin{aligned}
\text{Diagram 1} &= -i \frac{\eta_{\mu\nu}}{p^2} & \text{Diagram 2} &= \frac{i}{p^2} \\
\text{Diagram 3} &= \frac{i}{\sqrt{2}} (\eta_{\nu\rho}(p-q)_\mu - 2\eta_{\rho\mu}k_\nu + 2\eta_{\mu\nu}k_\rho) \\
\text{Diagram 4} &= -\frac{i}{2} \eta_{\mu\nu} \eta_{\rho\lambda} - i \eta_{\mu\lambda} \eta_{\nu\rho} + i \eta_{\mu\rho} \eta_{\nu\lambda} \\
\text{Diagram 5} &= \frac{i}{\sqrt{2}} (p-q)_\mu & \text{Diagram 6} &= -\frac{i}{2} \eta_{\mu\nu}
\end{aligned}$$

Figure 8: The color-ordered background-field Feynman gauge three- and four-point vertices. Dashed lines represent either ghosts or scalars.

bilinear in the quantum field A_μ^Q . These suffice for computing the one-loop effective action $\Gamma[A^B]$, since A_μ^Q describes the gluon propagating around the loop while A_μ^B describes a gluon emerging from the loop.

Any one-loop diagram can be split into a one-particle-irreducible (1PI) part, or loop part, along with a set of tree diagrams sewn onto the loop. Now, $\Gamma[A^B]$ is invariant with respect to A^B gauge transformations [40]. Therefore we may use *any* single gauge to compute the trees which are to be sewn onto the 1PI parts of the diagrams. Indeed, the string-motivated recipe is to use background-field gauge only for the 1PI or loop vertices, and Gervais-Neveu gauge for the remaining tree vertices [38]. This approach retains the above-noted advantages of Gervais-Neveu gauge for tree computations, while avoiding the complicated ghost interactions this nonlinear gauge would entail if it were used inside the loop. The advantage of the background-field gauge inside the loop is that the loop momentum appears in only the first term in the tri-linear gauge vertex in fig. 8; the last two terms contain only the external momentum k . (In general, the most complicated loop integrals to evaluate are those with the most insertions of the loop momentum in the numerator.) Furthermore, the first term matches the scalar-scalar-gluon vertex, up to the $\eta_{\nu\rho}$ factor. Thus in background-field gauge the leading loop-momentum behavior of one-particle-irreducible graphs with a gluon in the loop is very similar to that of graphs with a scalar in the loop. Note also that the interactions of a scalar and of a ghost with the background field are identical, up to the overall minus sign for a ghost

loop. In the next subsection we elaborate further on these relations.

3.2 Supersymmetric Decomposition

String theory suggests a natural decomposition of QCD amplitudes into supersymmetric and non-supersymmetric parts. For example, for an n -gluon one-loop amplitude the contributions of a fermion and of a gluon circulating in the loop can be decomposed as

$$\begin{aligned} A_{n;1}^{\text{fermion}} &= -A_{n;1}^{\text{scalar}} + A_{n;1}^{N=1}, \\ A_{n;1}^{\text{gluon}} &= A_{n;1}^{\text{scalar}} - 4A_{n;1}^{N=1} + A_{n;1}^{N=4}. \end{aligned} \quad (18)$$

Here the “scalar” superscript denotes the contribution of a complex scalar in the loop; the $N = 1$ superscript refers to the contribution of a $N = 1$ supersymmetric chiral multiplet, consisting of a complex scalar and a Weyl fermion; and the $N = 4$ label refers to a vector supermultiplet, consisting of three complex scalars, four Weyl fermions and a single gluon, all in the adjoint representation. (We have assumed the use of a supersymmetry preserving regulator [31, 28, 34, 30] in these equations, and the vector-multiplet loop is defined to include the ghost loop.)

The two supersymmetric components of eq. (18) have important cancellations in their leading loop-momentum behavior. The simplest way to see this is via the scalar, fermion and gluon loop contributions to the background-field effective action,

$$\begin{aligned} \Gamma^{\text{scalar}}[A] &= \ln \det_{[0]}^{-1} (D^2), \\ \Gamma^{\text{fermion}}[A] &= \frac{1}{2} \ln \det_{[1/2]}^{1/2} (D^2 - g \frac{1}{2} \sigma^{\mu\nu} F_{\mu\nu} / \sqrt{2}), \\ \Gamma^{\text{gluon}}[A] &= \ln \det_{[1]}^{-1/2} (D^2 - g \Sigma^{\mu\nu} F_{\mu\nu} / \sqrt{2}) + \ln \det_{[0]} (D^2), \end{aligned} \quad (19)$$

where $\frac{1}{2}\sigma_{\mu\nu}$ and $\Sigma_{\mu\nu}$ are respectively the spin- $\frac{1}{2}$ and spin-1 Lorentz generators, and where $\det_{[J]}$ is the one-loop determinant for a particle of spin J in the loop. The fermionic contribution has been rewritten in second-order form using

$$\begin{aligned} \ln \det_{[1/2]}^{1/2} (\not{D}) &= \frac{1}{2} \ln \det_{[1/2]}^{1/2} (\not{D}^2), \\ \not{D}^2 &= \frac{1}{2} \{ \not{D}, \not{D} \} + \frac{1}{2} [\not{D}, \not{D}] = D^2 - g \frac{1}{2} \sigma^{\mu\nu} F_{\mu\nu} / \sqrt{2}. \end{aligned} \quad (20)$$

In an m -point 1PI graph, the leading behavior of each contribution in eq. (19) for large loop momentum ℓ is ℓ^m . The leading term always

comes from the D^2 term in eq. (19), because $F_{\mu\nu}$ contains only the external momenta, not the loop momentum. Using $\text{Tr}_{[0]}(1) = 1$, $\text{Tr}_{[1/2]}(1) = \text{Tr}_{[1]}(1) = 4$, we see that the D^2 term cancels between the scalar and fermion loop, and between the fermion and gluon loop; hence it cancels in any supersymmetric linear combination. Subleading terms in supersymmetric combinations come from using one or more factors of F in generating a graph; each F costs one power of ℓ . Terms with a lone F vanish, thanks to $\text{Tr} \sigma_{\mu\nu} = \text{Tr} \Sigma_{\mu\nu} = 0$. This reduces the leading power in an m -point 1PI graph from ℓ^m down to ℓ^{m-2} . This argument can be extended to any amplitude in a supersymmetric gauge theory [15] and is related to the improved ultraviolet behavior of supersymmetric amplitudes. For the amplitude $A_{n;1}^{N=4}$, a comparison of the traces of products of two and three $\sigma_{\mu\nu}$'s and $\Sigma_{\mu\nu}$'s shows that further cancellations reduce the leading power behavior all the way down to ℓ^{m-4} . This result can also be derived by superspace techniques [42]. In a gauge other than Feynman background-field gauge, the cancellations involving the gluon loop would no longer happen diagram by diagram.

We illustrate the supersymmetric decomposition with the five-gluon amplitude, $A_{5;1}(1^-, 2^-, 3^+, 4^+, 5^+)$, whose components (18) are [22]

$$\begin{aligned}
A^{N=4} &= c_\Gamma A^{\text{tree}} \sum_{j=1}^5 \left[-\frac{1}{\epsilon^2} (-s_{j,j+1})^{-\epsilon} + \ln \left(\frac{-s_{j,j+1}}{-s_{j+1,j+2}} \right) \ln \left(\frac{-s_{j+2,j-2}}{-s_{j-2,j-1}} \right) + \frac{\pi^2}{6} \right], \\
A^{N=1} &= c_\Gamma A^{\text{tree}} \left[\frac{1}{\epsilon} - \frac{1}{2} [\ln(-s_{23}) + \ln(-s_{51})] + 2 \right] \\
&\quad + \frac{i c_\Gamma}{2} \frac{\langle 1 2 \rangle^2 (\langle 2 3 \rangle [3 4] \langle 4 1 \rangle + \langle 2 4 \rangle [4 5] \langle 5 1 \rangle)}{\langle 2 3 \rangle \langle 3 4 \rangle \langle 4 5 \rangle \langle 5 1 \rangle} \frac{\ln \left(\frac{-s_{23}}{-s_{51}} \right)}{s_{51} - s_{23}}, \\
A^{\text{scalar}} &= \frac{1}{3} A^{N=1} + \frac{2}{9} c_\Gamma A^{\text{tree}} - \frac{i c_\Gamma}{3} \\
&\times \left[\frac{[3 4] \langle 4 1 \rangle \langle 2 4 \rangle [4 5] (\langle 2 3 \rangle [3 4] \langle 4 1 \rangle + \langle 2 4 \rangle [4 5] \langle 5 1 \rangle)}{\langle 3 4 \rangle \langle 4 5 \rangle} \frac{\ln \left(\frac{-s_{23}}{-s_{51}} \right) - \frac{1}{2} \left(\frac{s_{23}}{s_{51}} - \frac{s_{51}}{s_{23}} \right)}{(s_{51} - s_{23})^3} \right. \\
&\quad \left. + \frac{\langle 3 5 \rangle [3 5]^3}{[1 2] [2 3] \langle 3 4 \rangle \langle 4 5 \rangle [5 1]} - \frac{\langle 1 2 \rangle [3 5]^2}{[2 3] \langle 3 4 \rangle \langle 4 5 \rangle [5 1]} - \frac{1}{2} \frac{\langle 1 2 \rangle [3 4] \langle 4 1 \rangle \langle 2 4 \rangle [4 5]}{s_{23} \langle 3 4 \rangle \langle 4 5 \rangle s_{51}} \right], \tag{21}
\end{aligned}$$

where

$$A^{\text{tree}} \equiv A_5^{\text{tree}}(1^-, 2^-, 3^+, 4^+, 5^+) = i \frac{\langle 1 2 \rangle^4}{\langle 1 2 \rangle \langle 2 3 \rangle \langle 3 4 \rangle \langle 4 5 \rangle \langle 5 1 \rangle}, \tag{22}$$

$$c_\Gamma \equiv \frac{r_\Gamma}{(4\pi)^{2-\epsilon}} \equiv \frac{\Gamma(1+\epsilon)\Gamma^2(1-\epsilon)}{(4\pi)^{2-\epsilon}\Gamma(1-2\epsilon)}. \quad (23)$$

These amplitudes contain both infrared and ultraviolet divergences, which have been regulated dimensionally with $D = 4 - 2\epsilon$, retaining terms through $\mathcal{O}(\epsilon^0)$. We see that the three components have quite different analytic structure, indicating that the rearrangement is a natural one. The $N = 4$ supersymmetric component is the simplest, followed by the $N = 1$ component. The non-supersymmetric scalar component is the most complicated, yet it is still simpler than the amplitude with a gluon circulating in the loop, because it does not mix all three components together. The amplitudes for the one other helicity configuration needed for NLO corrections, $A_{5;1}(1^-, 2^+, 3^-, 4^+, 5^+)$, are a bit more complicated [22].

The surprising simplicity of $N = 4$ supersymmetric loop amplitudes was first observed by Green, Schwarz and Brink in their calculation of the four-gluon amplitude as the low-energy limit of a superstring amplitude [43]. The supersymmetric decomposition can also reveal structure in electroweak amplitudes that would otherwise remain hidden [44]. As we shall discuss in section 4, the cancellation of leading powers of loop momentum for supersymmetric multiplets is extremely useful for constructing such amplitudes via unitarity [14, 15].

4 UNITARITY

Unitarity has been a useful tool in quantum field theory since its inception. The Cutkosky rules [45, 46] allow one to obtain the imaginary³ (absorptive) parts of one-loop amplitudes directly from products of tree amplitudes. This is generally much easier than a full diagrammatic calculation because one can greatly simplify the tree amplitudes *before* feeding them into the calculation of the cuts.

Having obtained the imaginary parts, one traditionally uses dispersion relations to reconstruct real (dispersive) parts, up to additive rational function ambiguities. Although the Cutkosky rules are computationally simpler than Feynman rules, the additive ambiguity has hampered their use in obtaining complete amplitudes. Here we show how this problem is alleviated by the supersymmetry decomposition of section 3, and by a complete knowledge of all functions that may enter into a calculation [47, 48].

³By imaginary we mean the discontinuities across branch cuts.

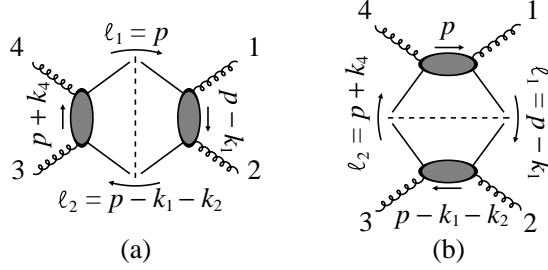


Figure 9: The s - and t -channel cuts of a one-loop four-gluon amplitude. The cut lines can be gluons, fermions, or scalars.

4.1 Cutkosky Rules

Consider the s -channel cut of the four-point amplitude represented pictorially in fig. 9a. The Mandelstam variables are as usual $s = (k_1 + k_2)^2$ and $t = (k_2 + k_3)^2$. According to the Cutkosky rules, the s -channel cut (with $s > 0$ and $t < 0$) of this amplitude is

$$\begin{aligned}
 -i \text{Disc } A_{4;1}(1, 2, 3, 4) \Big|_{s\text{-cut}} &= \int \frac{d^{4-2\epsilon} p}{(2\pi)^{4-2\epsilon}} 2\pi \delta^{(+)}(\ell_1^2) 2\pi \delta^{(+)}(\ell_2^2) \\
 &\quad \times A_4^{\text{tree}}(-\ell_1, 1, 2, \ell_2) A_4^{\text{tree}}(-\ell_2, 3, 4, \ell_1),
 \end{aligned}
 \tag{24}$$

where $\ell_1 = p$ and $\ell_2 = p - k_1 - k_2$, $\delta^{(+)}$ is the positive-energy branch of the delta-function and ‘Disc’ means the discontinuity across the branch cut. Color-ordering requires us to maintain the clockwise ordering of the legs in sewing the tree amplitudes.

Suppose the amplitude had the form $A_{4;1} = c \ln(-s) + \dots = c(\ln|s| - i\pi) + \dots$, where the coefficient c is a rational function. Then the phase space integral (24) would generate the $i\pi$ term but drop the $\ln|s|$ term. Since we wish to obtain both types of terms, real and imaginary, we replace the phase-space integral by the cut of an unrestricted loop momentum integral [14]; that is, we replace the δ -functions with Feynman propagators,

$$\begin{aligned}
 A_{4;1}(1, 2, 3, 4) \Big|_{s\text{-cut}} &= \\
 &\left[\int \frac{d^{4-2\epsilon} p}{(2\pi)^{4-2\epsilon}} \frac{i}{\ell_1^2} A_4^{\text{tree}}(-\ell_1, 1, 2, \ell_2) \frac{i}{\ell_2^2} A_4^{\text{tree}}(-\ell_2, 3, 4, \ell_1) \right] \Big|_{s\text{-cut}}.
 \end{aligned}
 \tag{25}$$

While eq. (24) includes only imaginary parts, eq. (25) contains both real and imaginary parts. As indicated, eq. (25) is valid only for those terms with an s -channel branch cut; terms without an s -channel cut may not be correct. A very useful property of this formula is that one may continue to use on-shell conditions for the cut intermediate legs inside the tree amplitudes without affecting the result. Only terms containing no cut in this channel would change. A similar equation holds for the t -channel cut depicted in fig. 9b. Combining the two cuts into a single function, one obtains the full amplitude, up to possible ambiguities in rational functions.

This procedure generalizes to an arbitrary number of external legs. Isolate the cut in a single momentum channel by taking exactly one of the momentum invariants to be above threshold, and the rest of the cyclicly adjacent ones to be negative (space-like). To construct all terms with cuts in an amplitude, combine the contributions from the various channels into a single function with the correct cuts in all channels. Below we describe how to link the rational functions appearing in amplitudes to terms with cuts, so that complete amplitudes can be obtained from Cutkosky rules.

4.2 *Cut Constructibility*

One-loop amplitudes satisfying a certain power-counting criterion (for example supersymmetric amplitudes) can be obtained directly from four-dimensional tree amplitudes via the Cutkosky rules. That is, when the criterion is satisfied, one may fix all rational functions appearing in the amplitudes directly from terms (through $\mathcal{O}(\epsilon^0)$) in the amplitudes which contain cuts. We refer to such amplitudes as ‘cut-constructible’. (Amplitudes not satisfying the criterion can still be obtained from cuts, but one must evaluate the cuts to higher order in ϵ , which is more work.) In the decomposition of $A_{5;1}$ given in eq. (21), the $N = 4$ and $N = 1$ supersymmetric components are cut-constructible, while the scalar component is not. Correspondingly, rational functions in the first two components (i.e., $\frac{\pi^2}{6}$ and 2) are intimately linked to the logarithms, while the last three rational terms in $A_{5;1}^{\text{scalar}}$ are not so linked.

In a one-loop calculation one encounters integrals of the form

$$\begin{aligned}\mathcal{I}_m[P(p^\mu)] &\equiv \int \frac{d^{4-2\epsilon}p}{(2\pi)^{4-2\epsilon}} \frac{P(p^\mu)}{p^2(p-K_1)^2(p-K_1-K_2)^2\cdots(p+K_m)^2} \\ &\equiv \frac{i(-1)^m}{(4\pi)^{2-\epsilon}} I_m[P(p^\mu)],\end{aligned}\tag{26}$$

where m is the number of propagators in the loop, K_i are sums of external momenta k_i , and $P(p^\mu)$ is the loop-momentum polynomial. A *cut-constructible* amplitude is one for which one can arrange that all the $P(p^\mu)$ have degree at most $m-2$, except for $m=2$ when P should be at most linear. Any amplitude satisfying this power-counting criterion can be fully reconstructed from its cuts (through $\mathcal{O}(\epsilon^0)$) [15]. The basic idea behind the proof is that only a restricted set of analytic functions appear in a cut-constructible amplitude. The standard Passarino-Veltman method [49] reduces the generic tensor integral $I_m[P(p^\mu)]$ to a linear combination of basic integrals with from 2 to m external legs. (The kinematics of the lower-point integrals are obtained by cancelling denominator factors in the original integral. In a diagrammatic representation of the integrals, this corresponds to pinching together adjacent external legs.) A key feature of Passarino-Veltman reduction is that integrals obeying the power-counting criterion can be reduced entirely to scalar integrals (integrals with $P=1$). The proof of cut-constructibility is then based on showing that the cuts provide sufficient information to fix the coefficients of all the scalar integrals. As we shall exemplify, amplitudes not satisfying the power-counting criterion contain additional rational functions, which spoil the argument.

As an illustration, any cut-constructible massless four-point amplitude must be given by a linear combination of the five scalar integrals depicted in fig. 10. (The triangle integral with legs 3 and 4 pinched is equal to the integral with legs 1 and 2 pinched in fig. 10b and is therefore not included in the figure; similarly, the one with 2 and 3 pinched is equal to the one in fig. 10c.) All these integrals can be generated by Passarino-Veltman reduction of a box Feynman diagram; the triangle and bubble integrals can also be generated from other Feynman diagrams. (Bubbles on external legs vanish in dimensional regularization, and are therefore not included.) The coefficients of the integrals are fixed by the cuts because each integral contains logarithms unique to it: the box contains the product $\ln(-s)\ln(-t)$, the triangles $\ln(-s)^2$ or $\ln(-t)^2$, and the two bubbles contain $\ln(-s)$ or $\ln(-t)$. Consequently no linear combination of these integrals with rational coefficients can be

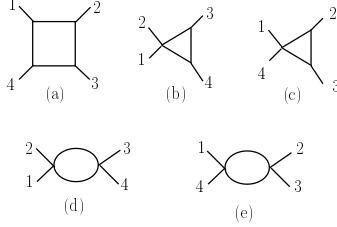


Figure 10: The independent scalar integrals that may appear in a massless four-point calculation.

formed which is cut-free.

The proof for an arbitrary number of external legs is similar, although more complicated. By systematically inspecting all scalar integrals that enter into an n -point amplitude, one may show that the cuts fix the coefficients of all integrals uniquely [15]. One may also show that the errors induced by ignoring the difference between using $D = 4 - 2\epsilon$ and $D = 4$ momenta on the cut legs do not affect the cuts through $\mathcal{O}(\epsilon^0)$. This observation is of considerable practical use because $D = 4$ tree amplitudes are simpler than those with legs in $D = 4 - 2\epsilon$.

The proof breaks down for amplitudes that do not satisfy the power-counting criterion. For example, the scalar bubble with momentum K ,

$$I_2[1](K) = \frac{r_\Gamma}{\epsilon(1-2\epsilon)}(-K^2)^{-\epsilon} = \frac{1}{\epsilon} + \ln(-K^2) + 2 + \mathcal{O}(\epsilon), \quad (27)$$

obeys the criterion. It contains a rational function, ‘2’, but the latter is always accompanied by $\ln(-K^2)$. On the other hand, the linear combination

$$\left(\frac{K^\mu K^\nu}{3} - \frac{\eta^{\mu\nu} K^2}{12}\right) I_2[1](K) - I_2[p^\mu p^\nu](K) = -\frac{1}{18}(K^\mu K^\nu - \eta^{\mu\nu} K^2) + \mathcal{O}(\epsilon) \quad (28)$$

does not obey the criterion, because $I_2[p^\mu p^\nu](K)$ is quadratic in the loop momentum. The combination (28) is free of cuts through $\mathcal{O}(\epsilon^0)$; there is no logarithm attached to it at this order. The presence of such a combination within an amplitude cannot be detected using the $\mathcal{O}(\epsilon^0)$ cuts.

In general, the power counting associated with a given amplitude depends on the specific gauge choice and diagrammatic organization. However, it suffices to find one organization of the diagrams satisfying the power-counting criterion. The string-inspired method discussed in

section 3 provides such an organization; it can satisfy the power-counting criterion even when the corresponding diagrams in conventional Feynman gauge do not. An important class of cut-constructible amplitudes are those in supersymmetric gauge theory. In section 3.2 we showed that for n -gluon amplitudes the leading two powers of loop momentum cancel in a supermultiplet contribution; the same result holds for amplitudes with external fermions [15].

4.3 Supersymmetric Examples

As a simple example, consider the contribution of an $N = 4$ supersymmetry multiplet to a four-gluon amplitude. This amplitude is an ordinary gauge-theory amplitude but with a particular matter content: one gluon, four gluinos and six real scalars all in the adjoint representation. As discussed in section 2.4, $A_{4;1}^{\text{SUSY}}(1^\pm, 2^+, 3^+, 4^+) = 0$ so the first non-trivial case to consider is $A_{4;1}^{N=4}(1^-, 2^-, 3^+, 4^+)$.

For the s -channel cut depicted in fig. 9, only the gluon loop contributes; for fermion or scalar loops the supersymmetry identities in eq. (14) guarantee that at least one of the two tree amplitudes vanish. The necessary tree amplitudes are the four-gluon amplitudes

$$\begin{aligned} A_4^{\text{tree}}(-\ell_1^+, 1^-, 2^-, \ell_2^+) &= i \frac{\langle 1 2 \rangle^4}{\langle -\ell_1 1 \rangle \langle 1 2 \rangle \langle 2 \ell_2 \rangle \langle \ell_2 - \ell_1 \rangle}, \\ A_4^{\text{tree}}(-\ell_2^-, 3^+, 4^+, \ell_1^-) &= i \frac{\langle -\ell_1 \ell_2 \rangle^4}{\langle -\ell_2 3 \rangle \langle 3 4 \rangle \langle 4 \ell_1 \rangle \langle \ell_1 - \ell_2 \rangle}. \end{aligned} \quad (29)$$

All other combinations of helicities of the intermediate lines cause at least one of the tree amplitudes on either side of the cut to vanish. (The outgoing-particle helicity convention means that the helicity label for each intermediate line flips when crossing the cut.) Cut-constructibility of supersymmetric amplitudes allows us to use the four-dimensional tree amplitudes, so that the cut in the s channel, eq. (25), becomes

$$\begin{aligned} A_{4;1}^{N=4}(1^-, 2^-, 3^+, 4^+) \Big|_{s\text{-cut}} &= \int \frac{d^{4-2\epsilon}p}{(2\pi)^{4-2\epsilon}} \frac{i}{\ell_1^2} \frac{i \langle 1 2 \rangle^4}{\langle \ell_1 1 \rangle \langle 1 2 \rangle \langle 2 \ell_2 \rangle \langle \ell_2 \ell_1 \rangle} \\ &\quad \times \frac{i}{\ell_2^2} \frac{i \langle \ell_1 \ell_2 \rangle^4}{\langle \ell_2 3 \rangle \langle 3 4 \rangle \langle 4 \ell_1 \rangle \langle \ell_1 \ell_2 \rangle} \Big|_{s\text{-cut}}, \end{aligned} \quad (30)$$

where we have removed the minus signs from inside the spinor products by cancelling constant phases. To put this integral into a form more

reminiscent of integrals encountered in Feynman diagram calculations we may rationalize the denominators using, for example,

$$\frac{1}{\langle 2 \ell_2 \rangle} = -\frac{[2 \ell_2]}{(p - k_1)^2}. \quad (31)$$

We use the on-shell conditions $\ell_1^2 = 0$ and $\ell_2^2 = 0$, which apply even though the loop integral is unrestricted, because of the s -cut restriction. Performing such simplifications yields,

$$\begin{aligned} & A_{4;1}^{N=4}(1^-, 2^-, 3^+, 4^+) \Big|_{s\text{-cut}} \\ &= -i A_4^{\text{tree}} \left[\int \frac{d^{4-2\epsilon} p}{(2\pi)^{4-2\epsilon}} \frac{\mathcal{N}}{p^2(p - k_1)^4(p - k_1 - k_2)^2(p + k_4)^4} \right] \Big|_{s\text{-cut}}, \end{aligned} \quad (32)$$

where we have extracted a factor of the tree amplitude,

$$A_4^{\text{tree}}(1^-, 2^-, 3^+, 4^+) = i \frac{\langle 1 2 \rangle^4}{\langle 1 2 \rangle \langle 2 3 \rangle \langle 3 4 \rangle \langle 4 1 \rangle}, \quad (33)$$

from the amplitude. The numerator of the integrand is

$$\begin{aligned} \mathcal{N} &= [\ell_1 1] \langle 1 4 \rangle [4 \ell_1] \langle \ell_1 \ell_2 \rangle [\ell_2 3] \langle 3 2 \rangle [2 \ell_2] \langle \ell_2 \ell_1 \rangle \\ &= \text{tr}_+[\ell_1 1 4 \ell_1 \ell_2 3 2 \ell_2] \\ &= -4 \text{tr}_+[4 3 2 1] \ell_1 \cdot k_1 \ell_1 \cdot k_4 = -st(p - k_1)^2(p + k_4)^2, \end{aligned} \quad (34)$$

where $\text{tr}_+[\dots] = \frac{1}{2} \text{tr}[(1 + \gamma_5) \dots]$ and we used

$$\ell_1^2 = 0, \quad \ell_1 \ell_2 = \ell_1 (\not{k}_3 + \not{k}_4), \quad \ell_2 \ell_1 = -(\not{k}_1 + \not{k}_2) \ell_1. \quad (35)$$

The γ_5 term in the trace drops out because a four-point amplitude has only three independent momenta to contract into the totally anti-symmetric Levi-Civita tensor.

Thus in eq. (32) the numerator neatly reduces the squared propagators to single propagators,

$$ist A_4^{\text{tree}} \int \frac{d^{4-2\epsilon} p}{(2\pi)^{4-2\epsilon}} \frac{1}{p^2(p - k_1)^2(p - k_1 - k_2)^2(p + k_4)^2} \Big|_{s\text{-cut}}, \quad (36)$$

which is a scalar box integral. Thus the s -cut contribution is given by

$$A_{4;1}^{N=4}(1^-, 2^-, 3^+, 4^+) \Big|_{s\text{-cut}} = \frac{-st}{(4\pi)^{2-\epsilon}} A_4^{\text{tree}} I_4(s, t) \Big|_{s\text{-cut}}, \quad (37)$$

where the massless scalar box integral is (see e.g. ref. [48])

$$I_4(s, t) = -\frac{2r_\Gamma}{st} \left\{ -\frac{1}{\epsilon^2} [(-s)^{-\epsilon} + (-t)^{-\epsilon}] + \frac{1}{2} \ln^2 \left(\frac{s}{t} \right) + \frac{\pi^2}{2} \right\} + \mathcal{O}(\epsilon). \quad (38)$$

The evaluation of the t -channel cut depicted in fig. 9 is similar, but a bit more involved since all particles in the multiplet contribute. However, after summing over the contribution of all particles, with the help of the SWI (14) and the Schouten identity (11), the integral appearing in the t -channel cut turns out to be the same as the one appearing in the s -channel cut in eq. (32).

Combining the s and t channel results, the amplitude must be

$$A_{4;1}^{N=4}(1^-, 2^-, 3^+, 4^+) = \frac{-st}{(4\pi)^{2-\epsilon}} A_4^{\text{tree}} I_4(s, t). \quad (39)$$

The rational function proportional to π^2 contained in the box integral (38) is fixed by the cuts since it appears in association with the logarithms in this function. Integrals having cuts in multiple channels, such as $I_4(s, t)$, provide a strong consistency check: their coefficients can be obtained via two or more separate cut calculations and the results must agree.

Following the same procedure one may evaluate the other nonvanishing $N = 4$ four-gluon amplitude, $A_{4;1}^{N=4}(1^-, 2^+, 3^-, 4^+)$, where the negative helicities are non-adjacent. Surprisingly, the same basic calculation can be easily extended to an arbitrary number of external legs for maximally helicity violating (MHV) amplitudes, those with two negative-helicity gluons and the remaining of positive helicity. (A special case is $A_{5;1}^{N=4}(1^-, 2^-, 3^+, 4^+, 5^+)$, given in eq. (21).) The cuts fall into two categories, depending on whether the external negative-helicity gluons are on the same or on opposite sides of the cut, as depicted in fig. 11. In either case the tree amplitudes on both sides of the cuts are given by the Parke-Taylor formula [50, 3],

$$\begin{aligned} A^{\text{tree}}(\ell_1^+, m_1^+, \dots, k^-, \dots, j^-, \dots, m_2^+, \ell_2^+) \\ = i \frac{\langle k j \rangle^4}{\langle \ell_1 m_1 \rangle \langle m_1, m_1+1 \rangle \cdots \langle m_2-1, m_2 \rangle \langle m_2 \ell_2 \rangle \langle \ell_2 \ell_1 \rangle}, \end{aligned} \quad (40)$$

where j and k are the two negative-helicity legs, or by formulæ related to eq. (40) by the SWI (14). The key to evaluating the cut integrals for an arbitrary number of external legs is that only two denominator factors in the tree amplitudes (40) contain the loop momentum (since

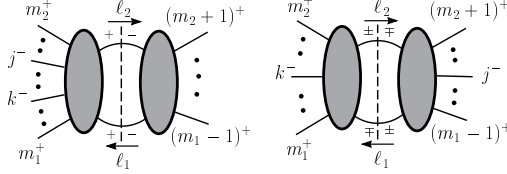


Figure 11: The relevant cuts for computing the MHV amplitudes for an arbitrary number of external legs.

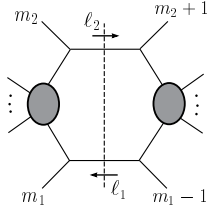


Figure 12: All- n MHV supersymmetric amplitudes can be evaluated by evaluating hexagon integrals.

$1/\langle \ell_2 \ell_1 \rangle = [\ell_2 \ell_1] / (k_{m_1} + \dots + k_{m_2})^2$). Thus each tree contributes only two propagators containing the loop momentum, so after including the two cut propagators the hardest integral to be evaluated is the hexagon integral depicted in fig. 12. These hexagon integrals can be reduced to scalar box integrals in much the same way as for the four-point case, allowing one to obtain the amplitudes for an arbitrary number of external legs [14].

The analysis of $N = 1$ supersymmetric MHV amplitudes is similar, although more complicated [15]. Again the key to the construction is that no more than six denominators contain loop momentum, even for an arbitrary number of external legs. One instance of the general $N = 1$ MHV result is provided by $A_{5;1}^{N=1}(1^-, 2^-, 3^+, 4^+, 5^+)$ in eq. (21). Notice that only the s_{23} and s_{51} channels contain cuts. This result (which is also true for the scalar component) is a simple consequence of the supersymmetry identities (14). The construction of amplitudes via cuts does not rely on supersymmetry, but only on the power-counting criterion; however, non-supersymmetric amplitudes generally do not satisfy the criterion.

4.4 Non-supersymmetric Example

Amplitudes not satisfying the power-counting criterion require an extension of this approach. Consider the non-supersymmetric amplitude for four identical helicity gluons with a scalar in the loop,

$$A_{4;1}^{\text{scalar}}(1^+, 2^+, 3^+, 4^+) = -\frac{i}{48\pi^2} \frac{[1\,2][3\,4]}{\langle 1\,2\rangle\langle 3\,4\rangle} + \mathcal{O}(\epsilon), \quad (41)$$

first obtained from string-based techniques [28]. At first sight one might think that it is impossible to use unitarity to obtain this amplitude, since it contains no cuts. The box Feynman diagram for this amplitude contains up to four powers of loop momentum, so the power-counting criterion is not satisfied (in any gauge).

However, in $D = 4 - 2\epsilon$ all terms in a massless amplitude necessarily have cuts [51]: by dimensional analysis of eq. (26), all terms must be proportional to factors of $(-K^2)^{-\epsilon}$, where K^2 is some kinematic variable. In particular a massless four-point amplitude must be of the form

$$\begin{aligned} A_4^{D=4-2\epsilon} &= (-s)^{-\epsilon} f_1 + (-t)^{-\epsilon} f_2 \\ &= (1 - \epsilon \ln(-s))f_1 + (1 - \epsilon \ln(-t))f_2 + \dots \end{aligned} \quad (42)$$

where f_1 and f_2 are dimensionless functions of the kinematic variables. This expression now contains cuts at $\mathcal{O}(\epsilon)$ even if f_1 and f_2 are cut-free. Rational functions such as those in eq. (41) may therefore be obtained from the sum $f_1 + f_2$, fixed by the coefficients of the single logarithms at $\mathcal{O}(\epsilon)$.

Thus, to obtain the rational function contributions in amplitudes which do not satisfy the power-counting criterion we must perform a cut calculation valid to at least one higher order in ϵ . We are not actually interested in the explicit values of the $\mathcal{O}(\epsilon)$ terms; we only need to extract the sum $f_1 + f_2$. To implement a calculation valid to higher orders in ϵ we correct for the fact that the loop momenta appearing in the tree amplitudes on either side of the cut are in $(4 - 2\epsilon)$ -dimensions instead of four-dimensions. The proper on-shell conditions on the cut legs are $\ell_1^2 - \mu^2 = 0$ and $\ell_2^2 - \mu^2 = 0$, where ℓ_1 and ℓ_2 are left in four-dimensions and μ is the (-2ϵ) -dimensional part of the loop momentum. We follow the standard prescription that the (-2ϵ) -dimensional subspace is orthogonal to the four-dimensional one [29]. For practical purposes we may think of μ^2 as a mass which gets integrated over. (This decomposition of the loop momentum has also been used by Mahlon [13] in his recursive approach.)

For the amplitude in eq. (41), the tree amplitudes entering the two sides of the s -channel cut, depicted in fig. 9a, are easily computed from color-ordered Feynman diagrams; the one on the left side of the cut is

$$A_4^{\text{tree}}(-\ell_1, 1^+, 2^+, \ell_2) = i\mu^2 \frac{[1\,2]}{\langle 1\,2 \rangle ((\ell_1 - k_1)^2 - \mu^2)}, \quad (43)$$

where legs ℓ_1 and ℓ_2 represent the cut scalar lines. The one on the right side is obtained by relabeling legs. The amplitude (43) vanishes in $D = 4$ ($\mu^2 \rightarrow 0$) by the SWI (14). Plugging these tree amplitudes into eq. (25), we obtain the s cut of the scalar loop contribution,

$$A_{4;1}^{\text{scalar}}(1^+, 2^+, 3^+, 4^+) \Big|_{s\text{-cut}} = 2 \frac{[1\,2][3\,4]}{\langle 1\,2 \rangle \langle 3\,4 \rangle} \mathcal{I}_4[\mu^4] \Big|_{s\text{-cut}}, \quad (44)$$

where the factor of 2 is from the two states of a complex scalar and

$$\mathcal{I}_4[\mu^4] \equiv \int \frac{d^4 p}{(2\pi)^4} \frac{d^{-2\epsilon} \mu}{(2\pi)^{-2\epsilon}} \frac{\mu^4}{(p^2 - \mu^2)((p - k_1)^2 - \mu^2) \cdots ((p + k_4)^2 - \mu^2)}. \quad (45)$$

The t -channel cut, depicted in fig. 9b, is similar and may be obtained via the relabeling $1 \leftrightarrow 3$. Using the identity

$$\frac{[3\,2][1\,4]}{\langle 3\,2 \rangle \langle 1\,4 \rangle} = \frac{[1\,2][3\,4]}{\langle 1\,2 \rangle \langle 3\,4 \rangle}, \quad (46)$$

the t -cut is given simply by eq. (44), with ‘ s -cut’ replaced by ‘ t -cut’.

Combining the two cuts we obtain an expression valid for both cuts,

$$A_{4;1}^{\text{scalar}}(1^+, 2^+, 3^+, 4^+) = 2 \frac{[1\,2][3\,4]}{\langle 1\,2 \rangle \langle 3\,4 \rangle} \mathcal{I}_4[\mu^4]. \quad (47)$$

Although we only calculated the cuts, we did so to all orders in ϵ ; therefore by eq. (42) we know the complete loop amplitude. To obtain the amplitude through $\mathcal{O}(\epsilon^0)$ we need only evaluate the leading $\mathcal{O}(\epsilon^0)$ contribution to the integral $\mathcal{I}_4[\mu^4]$.

A good way to evaluate the leading term is to first integrate out the angles in the (-2ϵ) -dimensional subspace. Using the fact that the integrand is a function only of μ^2 , we have

$$\int \frac{d^{-2\epsilon} \mu}{(2\pi)^{-2\epsilon}} \rightarrow -(4\pi)^\epsilon \frac{\epsilon}{\Gamma(1 - \epsilon)} \int_0^\infty d\mu^2 (\mu^2)^{-1-\epsilon}. \quad (48)$$

The overall ϵ from the measure must be compensated by a $1/\epsilon$ ultraviolet pole in the remaining integration. As usual a leading ultraviolet divergence may be extracted conveniently by setting all external momenta to

zero and inserting a mass parameter λ to replace the momenta. Thus we may evaluate the integral (45) as

$$\begin{aligned} \mathcal{I}_4[\mu^4] &\rightarrow \int \frac{d^4 p}{(2\pi)^4} \frac{d^{-2\epsilon} \mu}{(2\pi)^{-2\epsilon}} \frac{\mu^4}{(p^2 - \mu^2 - \lambda^2)^4} \\ &= -\frac{i\epsilon}{(4\pi)^{2-\epsilon}} \frac{1}{\Gamma(1-\epsilon)} \int_0^\infty dp^2 \int_0^\infty d\mu^2 \frac{p^2 (\mu^2)^{1-\epsilon}}{(p^2 + \mu^2 + \lambda^2)^4} \quad (49) \\ &= -\frac{i\epsilon}{(4\pi)^{2-\epsilon}} \left(\frac{1}{6\epsilon} + \mathcal{O}(1) \right), \end{aligned}$$

where we have used standard formulas [46] for the angular integrals and then integrated the radial dimension. Plugging the leading-in- ϵ result into eq. (47), we obtain the correct result for the amplitude (41).

Although this method can in principle be applied to any massless one-loop amplitude to obtain complete amplitudes, it is generally advantageous to first decompose amplitudes into pieces which are cut-constructible and pieces which are not. One may also calculate loop amplitudes for massive particles in this way [52], but cut-free integrals may appear. The coefficients of these functions must be determined by other means, such as knowledge of ultraviolet or infrared divergences.

5 FACTORIZATION

In quantum field theory, amplitudes are constrained by their behavior as kinematic variables vanish; they must factorize into a product of two amplitudes with an intermediate propagator. This may be used as a check on five- or higher-point amplitudes. (Factorization of four-point amplitudes in a theory without massive particles is trivial since the limiting kinematics is degenerate.) Factorization properties may also be used to help construct new amplitudes from known ones. In principle, this can be an extremely efficient way to obtain amplitudes since one avoids evaluating loop integrals.

Mangano and Parke have reviewed the factorization properties of tree-level QCD amplitudes [3]. We shall focus on the corresponding properties at one loop, which are a bit more complicated since the amplitudes generally contain infrared divergent pieces which do not factorize naively. Nevertheless, as any kinematic variable vanishes, one-loop amplitudes have a universal behavior quite similar to that of tree-level amplitudes.

5.1 General Framework

First we review briefly the situation at tree level. Color-ordered amplitudes can have poles only in channels corresponding to the sum of *cyclicly adjacent* momenta, that is as $P_{i,j}^2 \rightarrow 0$, where $P_{i,j}^\mu \equiv (k_i + k_{i+1} + \dots + k_j)^\mu$. This is because singularities arise from propagators going on-shell, and propagators for color-ordered graphs always carry momenta of the form $P_{i,j}^\mu$. The general form of an n -point color-ordered tree amplitude in the limit that $P_{1,m}^2$ vanishes is

$$A_n^{\text{tree}}(1, \dots, n) \xrightarrow{P_{1,m}^2 \rightarrow 0} \sum_{\lambda=\pm} A_{m+1}^{\text{tree}}(1, \dots, m, P^\lambda) \frac{i}{P_{1,m}^2} A_{n-m+1}^{\text{tree}}(m+1, \dots, n, P^{-\lambda}), \quad (50)$$

where $P_{1,m}$ is the intermediate momentum, A_{m+1}^{tree} and A_{n-m+1}^{tree} are lower-point scattering amplitudes, and λ denotes the helicity of the intermediate state P . The intermediate helicity is reversed going from one product amplitude to the other because of the outgoing-particle helicity convention.

For two-particle channels ($m = 2$), eq. (50) needs to be modified, because a three-point massless scattering amplitude is not kinematically possible. As $P_{12}^2 \rightarrow 0$, k_1 and k_2 become collinear. QCD amplitudes have an angular-momentum obstruction in this limit. For example, a gluon of helicity $+1$ cannot split into two collinear helicity ± 1 gluons and conserve angular momentum. This transforms the full pole in $P_{12}^2 = s_{12}$ into the square-root of a pole, $1/\sqrt{s_{12}}$, a behavior which is well captured via the spinor products $\langle 12 \rangle, [12]$. It is useful to lump all terms not associated with A_{n-1}^{tree} in eq. (50) into a ‘splitting amplitude’ $\text{Split}^{\text{tree}}$. In particular, as the momenta of adjacent legs a and b become collinear, we have

$$A_n^{\text{tree}}(\dots, a^{\lambda_a}, b^{\lambda_b}, \dots) \xrightarrow{a\parallel b} \sum_{\lambda=\pm} \text{Split}_{-\lambda}^{\text{tree}}(z, a^{\lambda_a}, b^{\lambda_b}) A_{n-1}^{\text{tree}}(\dots, P^\lambda, \dots), \quad (51)$$

where P is the intermediate state with momentum $k_P = k_a + k_b$, λ denotes the helicity of P , and z is the longitudinal momentum fraction, $k_a \approx z k_P$, $k_b \approx (1-z) k_P$. The universality of these limits can be derived diagrammatically, but an elegant way to derive it is from string theory [3], because all the field theory diagrams on each side of the pole are lumped into one string diagram.

Given the general form (51), one may obtain explicit expressions for the tree-level $g \rightarrow gg$ splitting amplitudes from the four- and five-gluon

amplitudes [53, 3, 21]. For example, taking the collinear limits of eq. (22) for $A_5^{\text{tree}}(1^-, 2^-, 3^+, 4^+, 5^+)$ and comparing to eqs. (33) and (51) shows that

$$\begin{aligned}\text{Split}_-^{\text{tree}}(a^-, b^-) &= 0, \\ \text{Split}_-^{\text{tree}}(a^+, b^+) &= \frac{1}{\sqrt{z(1-z)} \langle ab \rangle}, \\ \text{Split}_+^{\text{tree}}(a^+, b^-) &= \frac{(1-z)^2}{\sqrt{z(1-z)} \langle ab \rangle}, \\ \text{Split}_+^{\text{tree}}(a^-, b^+) &= \frac{z^2}{\sqrt{z(1-z)} \langle ab \rangle}.\end{aligned}\tag{52}$$

The remaining helicity configurations are obtained using parity. The $g \rightarrow \bar{q}q$ and $q \rightarrow qg$ splitting amplitudes can be obtained in similar fashion.

The situation for color-ordered one-loop amplitudes is similar to tree level. The one-loop analog of eq. (50) is schematically depicted in fig. 13, and is given by

$$\begin{aligned}A_n^{\text{loop}}(1, \dots, n) &\xrightarrow{P_{1,m}^2 \rightarrow 0} \\ &\sum_{\lambda=\pm} \left[A_{m+1}^{\text{loop}}(1, \dots, m, P^\lambda) \frac{i}{P_{1,m}^2} A_{n-m+1}^{\text{tree}}(m+1, \dots, n, P^{-\lambda}) \right. \\ &\quad + A_{m+1}^{\text{tree}}(1, \dots, m, P^\lambda) \frac{i}{P_{1,m}^2} A_{n-m+1}^{\text{loop}}(m+1, \dots, n, P^{-\lambda}) \\ &\quad \left. + A_{m+1}^{\text{tree}}(1, \dots, m, P^\lambda) \frac{i \text{Fact}_n(1, \dots, n)}{P_{1,m}^2} A_{n-m+1}^{\text{tree}}(m+1, \dots, n, P^{-\lambda}) \right],\end{aligned}\tag{53}$$

where the one-loop *factorization function*, Fact_n , is independent of helicities and does not cancel the pole in $P_{1,m}^2$. In an infrared divergent theory, such as QCD, amplitudes do not factorize ‘naively’: Fact_n may contain logarithms of kinematic invariants built out of momenta from *both* sides of the pole in $P_{1,m}^2$; $\ln(-s_{n,1})$ is an example of such a logarithm. The factorization functions are nonetheless universal functions depending on the infrared divergences present in the amplitudes [54].

The collinear limits for color-ordered one-loop amplitudes are a spe-

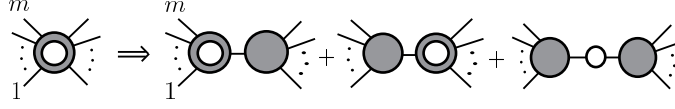


Figure 13: A schematic representation of the behavior of one-loop amplitudes as a kinematic invariant vanishes.

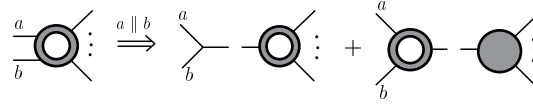


Figure 14: A schematic representation of the behavior of one-loop amplitudes as the momenta of two legs become collinear.

cial case and have the form

$$A_n^{\text{loop}} \xrightarrow{a \parallel b} \sum_{\lambda=\pm} \left(\text{Split}_{-\lambda}^{\text{tree}}(z, a^{\lambda_a}, b^{\lambda_b}) A_{n-1}^{\text{loop}}(\dots (a+b)^\lambda \dots) \right. \\ \left. + \text{Split}_{-\lambda}^{\text{loop}}(z, a^{\lambda_a}, b^{\lambda_b}) A_{n-1}^{\text{tree}}(\dots (a+b)^\lambda \dots) \right), \quad (54)$$

which is schematically depicted in fig. 14. The splitting amplitudes $\text{Split}_{-\lambda}^{\text{tree}}(a^{\lambda_a}, b^{\lambda_b})$ and $\text{Split}_{-\lambda}^{\text{loop}}(a^{\lambda_a}, b^{\lambda_b})$ are universal: they depend only on the two momenta becoming collinear, and not upon the specific amplitude under consideration. The explicit $\text{Split}_{-\lambda}^{\text{loop}}(a^{\lambda_a}, b^{\lambda_b})$ were originally determined from the four- and five-point one-loop amplitudes [22, 24] in much the same way as we obtained the tree-level splitting amplitudes above. (See appendix B of ref. [14].) Soft limits — the behavior as any particular $k_i \rightarrow 0$ — are also useful for constraining the form of one-loop amplitudes, and have a form analogous to eq. (54).

In performing explicit calculations, factorization provides an extremely stringent check since one must obtain the correct limits in all channels. A sign or labeling error, for example, will invariably be detected in some limits. In some cases one can also use factorization to construct ansätze for higher-point amplitudes [12, 14]. One writes down a sufficiently general form for a higher-point amplitude, containing arbitrary coefficients which are then fixed by imposing the correct behavior as kinematic variables vanish. A collinear bootstrap of this form would, however, miss functions that are nonsingular in all collinear limits. For

five-point amplitudes it is possible to write down such a function, namely

$$\frac{\varepsilon(1, 2, 3, 4)}{\langle 1\,2\rangle\langle 2\,3\rangle\langle 3\,4\rangle\langle 4\,5\rangle\langle 5\,1\rangle}, \quad (55)$$

since the contracted antisymmetric tensor $\varepsilon(1, 2, 3, 4) \equiv 4i\varepsilon_{\mu\nu\rho\sigma}k_1^\mu k_2^\nu k_3^\rho k_4^\sigma$ vanishes when any two of the five vectors k_i become collinear (using $\sum_{i=1}^5 k_i = 0$). However, it is quite possible that the factorization constraint uniquely specifies the rational functions of color-ordered $n \geq 6$ -point amplitudes, given the lower point amplitudes. A heuristic explanation of this conjecture is that as the number of external legs increases, by dimensional analysis the amplitudes require ever increasing powers of momenta in the denominators. Thus one expects more kinematic poles from the denominator than zeros from the numerator. We know of no counter-examples to this conjecture, but don't have a proof either.

5.2 Examples

As an example of the behavior of a one-loop amplitude in a collinear limit, consider the $N = 4$ five-gluon amplitude $A_{5;1}^{N=4}$ given in eq. (21). Taking the limit $k_4 \rightarrow zP$, $k_5 \rightarrow (1-z)P$, and using the four-gluon result (39), we find

$$\begin{aligned} A_{5;1}^{N=4}(1^-, 2^-, 3^+, 4^+, 5^+) &\xrightarrow{4||5} \text{Split}_-^{\text{tree}}(4^+, 5^+) A_{4;1}^{N=4}(1^-, 2^-, 3^+, P^+) \\ &\quad + \text{Split}_-^{N=4}(4^+, 5^+) A_4^{\text{tree}}(1^-, 2^-, 3^+, P^+), \end{aligned} \quad (56)$$

where the tree splitting amplitude is given in eq. (52). This limit determines the one-loop $N = 4$ multiplet contribution to the $g \rightarrow gg$ splitting amplitude,

$$\begin{aligned} \text{Split}_-^{N=4}(a^+, b^+) &= \\ c_\Gamma \text{Split}_-^{\text{tree}}(a^+, b^+) &\left[-\frac{1}{\epsilon^2} (-s_{ab} z(1-z))^{-\epsilon} + 2 \ln z \ln(1-z) - \frac{\pi^2}{6} \right]. \end{aligned} \quad (57)$$

Note that the loop splitting amplitude has absorbed the mismatch of infrared divergences between the five- and four-point amplitudes. This splitting amplitude will reappear in different collinear limits of this and other amplitudes.

Given the splitting amplitudes and five-point amplitudes, it is also possible to construct conjectures for higher-point amplitudes by demanding that they factorize correctly. Consider, for example, the complex-

scalar loop contribution to a five-gluon amplitude with all identical helicities [22],

$$A_{5;1}^{\text{scalar}}(1^+, 2^+, 3^+, 4^+, 5^+) = \frac{i}{96\pi^2} \frac{s_{12}s_{23} + s_{23}s_{34} + s_{34}s_{45} + s_{45}s_{51} + s_{51}s_{12} + \varepsilon(1, 2, 3, 4)}{\langle 1\,2 \rangle \langle 2\,3 \rangle \langle 3\,4 \rangle \langle 4\,5 \rangle \langle 5\,1 \rangle}. \quad (58)$$

As noted in section 3.2, for this helicity configuration the gluon and fermion loops are proportional to the scalar-loop contribution. One can verify that this amplitude has the correct collinear limits (54), using the four-gluon amplitude (41).

Using eq. (54), the explicit form of the tree splitting amplitudes (52), $A_n^{\text{tree}}(1^\pm, 2^+, \dots, n^+) = 0$, and experimenting at small n , we can construct higher-point amplitudes by writing down general forms with only two-particle poles, and requiring that they have the correct collinear limits. Doing so leads to the all- n ansatz [12],

$$A_{n;1}^{\text{scalar}}(1^+, 2^+, \dots, n^+) = -\frac{i}{48\pi^2} \sum_{1 \leq i_1 < i_2 < i_3 < i_4 \leq n} \frac{\text{tr}_-[i_1 i_2 i_3 i_4]}{\langle 1\,2 \rangle \langle 2\,3 \rangle \dots \langle n\,1 \rangle}, \quad (59)$$

where $\text{tr}_-[i_1 i_2 i_3 i_4] = \frac{1}{2} \text{tr}_-[(1 - \gamma_5) \not{k}_{i_1} \not{k}_{i_2} \not{k}_{i_3} \not{k}_{i_4}]$. This result has been confirmed by Mahlon via recursive techniques [13].

Indeed, the infinite sequence of one-loop $N = 4$ supersymmetric MHV amplitudes was first constructed via a collinear bootstrap and only then calculated using the unitarity method described in section 4.3. Other helicity configurations are more complicated, due to the appearance of multi-particle poles. Nevertheless, one can construct some six-point amplitudes from knowledge of the five-point amplitudes. This is most useful for the rational-function parts, which can be obtained via unitarity only by working to higher order in ϵ .

6 CONCLUSIONS AND OUTLOOK

We have reviewed various developments in calculational techniques for one-loop gauge theory amplitudes, especially in QCD. Such calculations are necessary in order to confront theoretical predictions with experiments to some degree of precision. Feynman rules, however, become extremely cumbersome for one-loop multi-parton calculations. Even the simplest processes are rather difficult to calculate without aid of a computer and for five or more external legs traditional methods break down

because of an exponential explosion in algebra. The results, however, are usually quite compact, especially when compared to intermediate expressions.

The computational situation can be greatly improved by combining a number of ideas. Methods that have previously been used at tree-level, such as spinor helicity [16], color decomposition [17], and supersymmetry Ward identities [18, 19], remain very useful at one loop. String theory motivates a number of improved organizational ideas such as supersymmetric decompositions, relations between color-decomposed amplitudes and improved gauge choices [28, 38, 32, 34]. These ideas mesh nicely with the use of Cutkosky rules [45] to obtain complete amplitudes. In the superstring organization of the amplitude, components can be identified whose rational as well as cut-containing parts can be obtained directly from knowledge of the branch cuts [14, 15]. The remaining components, though more difficult, can be attacked either by evaluating cuts to higher order in ϵ or by exploiting universal factorization properties [12].

The techniques discussed in this review have made possible a variety of new calculations, including those of all five-parton amplitudes [22, 23, 24] and of certain infinite sequences of massless amplitudes. The methods have also been applied to amplitudes containing massive particles [44, 52] and to gravitational amplitudes [33]. Mahlon has also used recursion relations, outside of the scope of this review, to obtain infinite sequences of fermion loop amplitudes with maximal helicity violation [13].

It would be desirable to extend these techniques to two-loop multi-parton calculations; while various authors have taken first steps [51, 37, 55, 56] in this direction, a great deal of work remains to be done.

We thank G. Chalmers, A.G. Morgan and especially D.C. Dunbar for collaboration on work described in this review. This work was supported in part by the US Department of Energy under grants DE-FG03-91ER40662 and DE-AC03-76SF00515, by the Alfred P. Sloan Foundation under grant BR-3222, and by the *Direction des Sciences de la Matière* of the *Commissariat à l'Energie Atomique* of France.

References

- [1] Particle Data Group, *Review of Particle Properties*, Phys. Rev. D50:1173 (1994) (page 1304); P. Langacker, in *Precision Tests of the Standard Electroweak Model*, ed. P. Langacker, (World Scientific, Singapore, 1994); G. Altarelli, preprint CERN-TH-7464-94, to appear in *Proceedings of International Symposium on Radiative Corrections: Status and Outlook*.
- [2] D. Gross and F. Wilczek, Phys. Rev. Lett. 30:1343 (1973); H.D. Politzer, Phys. Rev. Lett. 30:1346 (1973).
- [3] M. Mangano and S.J. Parke, Phys. Rep. 200:301 (1991).
- [4] A.D. Martin, W.J. Stirling, and R.G. Roberts, Phys. Lett. B306:145 (1993); err. *ibid.* B309:492 (1993).
- [5] CDF Collaboration, Fermilab preprint Fermilab-Conf-95-192-E, presented at the 10th Topical Workshop on Proton-Antiproton Collider Physics, Batavia, IL, May 9-13, 1995.
- [6] S.G. Gorishny, A.L. Kataev and S.A. Larin, Phys. Lett. B259:144 (1991); L.R. Surguladze and M.A. Samuel, Phys. Rev. Lett. 66:560 (1991); erratum *ibid.* 66:2416 (1991).
- [7] S.A. Larin, F.V. Tkachev and J.A.M. Vermaseren, Phys. Rev. Lett. 66:862 (1991); S.A. Larin and J.A.M. Vermaseren, Phys. Lett. B259:345 (1991).
- [8] S. Bethke, Nucl. Phys. B (Proc. Suppl.) 39B,C:198 (1995).
- [9] T. Kinoshita, J. Math. Phys. 3:650 (1962); T.D. Lee and M. Nauenberg, Phys. Rev. 133:B1549 (1964).
- [10] J.C. Collins, D.E. Soper, and G. Sterman, in *Perturbative Quantum Chromodynamics*, ed. A.H. Mueller (World Scientific, 1989).
- [11] S.D. Ellis, Z. Kunszt and D.E. Soper, Phys. Rev. D40:2188 (1989); Phys. Rev. Lett. 64:2121 (1990); Phys. Rev. Lett. 69:1496 (1992); F. Aversa, M. Greco, P. Chiappetta and J.P. Guillet, Phys. Rev. Lett. 65:401 (1990); F. Aversa, L. Gonzales, M. Greco, P. Chiappetta and J.P. Guillet, Z. Phys. C49:459 (1991); Z. Kunszt and D.E. Soper, Phys. Rev. D46:192 (1992); W.T. Giele and E.W.N. Glover, Phys. Rev. D46:1980 (1992); W.T. Giele, E.W.N. Glover and D.A. Kosower, Nucl. Phys. B403:633 (1993).

- [12] Z. Bern, L. Dixon and D.A. Kosower, *Proceedings of Strings 1993*, eds. M.B. Halpern, A. Sevrin and G. Rivlis (World Scientific, Singapore, 1994), hep-th/9311026; Z. Bern, G. Chalmers, L. Dixon and D.A. Kosower, Phys. Rev. Lett. 72:2134 (1994), hep-ph/9312333.
- [13] G.D. Mahlon, Phys. Rev. D49:2197 (1994); Phys. Rev. D49:4438 (1994).
- [14] Z. Bern, L. Dixon, D.C. Dunbar and D.A. Kosower, Nucl. Phys. B425:217 (1994), hep-ph/9403226.
- [15] Z. Bern, L. Dixon, D.C. Dunbar and D.A. Kosower, Nucl. Phys. B435:59 (1995), hep-ph/9409265.
- [16] F.A. Berends, R. Kleiss, P. De Causmaecker, R. Gastmans and T. T. Wu, Phys. Lett. 103B:124 (1981); P. De Causmaecker, R. Gastmans, W. Troost and T.T. Wu, Nucl. Phys. B206:53 (1982); R. Kleiss and W.J. Stirling, Nucl. Phys. B262:235 (1985); J.F. Gunion and Z. Kunszt, Phys. Lett. 161B:333 (1985); Z. Xu, D.-H. Zhang and L. Chang, Nucl. Phys. B291:392 (1987).
- [17] J.E. Paton and H.-M. Chan, Nucl. Phys. B10:519 (1969); P. Cvitanovic, P.G. Lauwers, and P.N. Scharbach, Nucl. Phys. B186:165 (1981); F.A. Berends and W.T. Giele, Nucl. Phys. B294:700 (1987); M. Mangano, S. Parke and Z. Xu, Nucl. Phys. B298:653 (1988); M. Mangano, Nucl. Phys. B309:461 (1988); D. Zeppenfeld, Int. J. Mod. Phys. A3:2175 (1988).
- [18] M.T. Grisaru, H.N. Pendleton and P. van Nieuwenhuizen, Phys. Rev. D15:996 (1977); M.T. Grisaru and H.N. Pendleton, Nucl. Phys. B124:81 (1977).
- [19] S.J. Parke and T. Taylor, Phys. Lett. 157B:81 (1985); Z. Kunszt, Nucl. Phys. B271:333 (1986).
- [20] F.A. Berends and W.T. Giele, Nucl. Phys. B306:759 (1988); D.A. Kosower, Nucl. Phys. B335:23 (1990); G. Mahlon and T.-M. Yan, Phys. Rev. D47:1776 (1993), hep-ph/9210213; G. Mahlon, Phys. Rev. D47:1812 (1993), hep-ph/9210214; G. Mahlon, T.-M. Yan and C. Dunn, Phys. Rev. D48:1337 (1993), hep-ph/9210212.
- [21] L. Dixon, preprint hep-ph/9601359, to appear in *Proceedings of Theoretical Advanced Study Institute in Elementary Particle Physics (TASI 95)*, ed. D.E. Soper.

- [22] Z. Bern, L. Dixon and D.A. Kosower, Phys. Rev. Lett. 70:2677 (1993).
- [23] Z. Kunszt, A. Signer and Z. Trócsányi, Phys. Lett. B336:529 (1994), hep-ph/9405386.
- [24] Z. Bern, L. Dixon and D.A. Kosower, Nucl. Phys. B437:259 (1995), hep-ph/9409393.
- [25] S. Frixione, Z. Kunszt and A. Signer, preprint hep-ph/9512328.
- [26] G. 't Hooft, Nucl. Phys. B72:461 (1974); Nucl. Phys. B75:461 (1974); P. Cvitanović, *Group Theory* (Nordita, 1984).
- [27] Z. Bern and D.A. Kosower, Nucl. Phys. B362:389 (1991).
- [28] Z. Bern and D.A. Kosower, Nucl. Phys. 379:451 (1992).
- [29] J.C. Collins, *Renormalization*, (Cambridge University Press) (1984).
- [30] Z. Kunszt, A. Signer and Z. Trócsányi, Nucl. Phys. B411:397 (1994).
- [31] W. Siegel, Phys. Lett. 84B:193 (1979); D.M. Capper, D.R.T. Jones and P. van Nieuwenhuizen, Nucl. Phys. B167:479 (1980).
- [32] Z. Bern and D.A. Kosower, Phys. Rev. Lett. 66:1669 (1991); Z. Bern and D.A. Kosower, in *Proceedings of the PASCOS-91 Symposium*, eds. P. Nath and S. Reucroft (World Scientific, 1992); Z. Bern, Phys. Lett. 296B:85 (1992); A. Pasquinucci and K. Roland, Nucl. Phys. B440:441 (1995), hep-th/9411015.
- [33] Z. Bern, D.C. Dunbar and T. Shimada, Phys. Lett. 312B:277 (1993), hep-th/9307001; D.C. Dunbar and P.S. Norridge, Nucl. Phys. B433:181 (1995), hep-th/9408014; preprint hep-th/9512084.
- [34] Z. Bern, hep-ph/9304249, in *Proceedings of Theoretical Advanced Study Institute in High Energy Physics (TASI 92)*, eds. J. Harvey and J. Polchinski (World Scientific, 1993).
- [35] C.S. Lam, Nucl. Phys. B397:143 (1993); Phys. Rev. D48:873 (1993).
- [36] M.J. Strassler, Nucl. Phys. B385:145 (1992); M.G. Schmidt and C. Schubert, Phys. Lett. 318B:438 (1993); Phys. Lett. B331:69 (1994); D. Fliegner, M.G. Schmidt and C. Schubert, Z. Phys. C64:111

- (1994), hep-ph/9401221; K. Daikouji, M. Shino and Y. Sumino, preprint hep-ph/9508377; M. Mondragon, L. Nellen, M.G. Schmidt and C. Schubert, Phys. Lett. B351:200 (1995), hep-th/9502125; preprint hep-th/9510036; E. D'Hoker and D.G. Gagne, preprint hep-th/9508131; preprint hep-th/9512080; H.-T. Sato, preprint hep-th/9511158.
- [37] M.G. Schmidt and C. Schubert, Phys. Lett. B331:69 (1994), hep-th/9403158; Nucl. Phys. B, Proc. Suppl. 39BC:306 (1995), hep-ph/9408394.
- [38] Z. Bern and D.C. Dunbar, Nucl. Phys. B379:562 (1992);
- [39] J.L. Gervais and A. Neveu, Nucl. Phys. B46:381 (1972).
- [40] G. 't Hooft, in Acta Universitatis Wratislavenensis no. 38, 12th Winter School of Theoretical Physics in Karpacz; *Functional and Probabilistic Methods in Quantum Field Theory*, Vol. 1 (1975); B.S. DeWitt, in Quantum gravity II, eds. C. Isham, R. Penrose and D. Sciama (Oxford, 1981); L.F. Abbott, Nucl. Phys. B185:189 (1981); L.F. Abbott, M.T. Grisaru and R.K. Schaefer, Nucl. Phys. B229:372 (1983).
- [41] R.P. Feynman and M. Gell-Mann, Phys. Rev. 109:193 (1958); J.L. Cortes, J. Gamboa and L. Velazquez, Phys. Lett. B313:108 (1993), hep-th/9301071; A.G. Morgan, Phys. Lett. B351:249 (1995), hep-ph/9502230.
- [42] S.J. Gates, M.T. Grisaru, M. Rocek and W. Siegel, *Superspace*, (Benjamin/Cummings, 1983).
- [43] M.B. Green, J.H. Schwarz and L. Brink, Nucl. Phys. B198:474 (1982).
- [44] E.W.N. Glover and A.G. Morgan, Z. Phys. C60:175 (1993); Z. Bern and A.G. Morgan, Phys. Rev. D49:6155 (1994), hep-ph/9312218.
- [45] L.D. Landau, Nucl. Phys. 13:181 (1959); S. Mandelstam, Phys. Rev. 112:1344 (1958), 115:1741 (1959); R.E. Cutkosky, J. Math. Phys. 1:429 (1960).
- [46] M.E. Peskin and D.V. Schroeder, *An Introduction to Quantum Field Theory* (Addison-Wesley, 1995).

- [47] B. Petersson, J. Math. Phys. 6:1955 (1965); G. Källén and J.S. Toll, J. Math. Phys. 6:299 (1965); D.B. Melrose, Il Nuovo Cimento 40A:181 (1965) G. 't Hooft and M. Veltman, Nucl. Phys. B153:365 (1979); W. van Neerven and J.A.M. Vermaseren, Phys. Lett. 137B:241 (1984); G.J. van Oldenborgh and J.A.M. Vermaseren, Zeit. Phys. C46:425 (1990); A. Denner, U. Nierste and R. Scharf, Nucl. Phys. B367:637 (1991).
- [48] Z. Bern, L. Dixon and D.A. Kosower, Phys. Lett. 302B:299 (1993); erratum *ibid.* 318B:649 (1993); Z. Bern, L. Dixon and D.A. Kosower, Nucl. Phys. B412:751 (1994), hep-ph/9306240.
- [49] L.M. Brown and R.P. Feynman, Phys. Rev. 85:231 (1952); L.M. Brown, Nuovo Cimento 21:3878 (1961); G. Passarino and M. Veltman, Nucl. Phys. B160:151 (1979).
- [50] S.J. Parke and T.R. Taylor, Phys. Rev. Lett. 56:2459 (1986).
- [51] W.L. van Neerven, Nucl. Phys. B268:453 (1986).
- [52] Z. Bern and A.G. Morgan, preprint hep-ph/9511336, to appear in Nucl. Phys. B.
- [53] F.A. Berends and W.T. Giele, Nucl. Phys. B313:595 (1989).
- [54] Z. Bern and G. Chalmers, Nucl. Phys. B447:465 (1995), hep-ph/9503236; G. Chalmers, hep-ph/9405393, in *Proceedings of the XXII ITEP International Winter School of Physics* (Gordon and Breach, 1995).
- [55] K. Roland, Phys. Lett. 289B:148 (1992); G. Cristofano, R. Marotta and K. Roland, Nucl. Phys. B392:345 (1993); A. Pasquinucci and K. Roland, Nucl. Phys. B457:27 (1995), hep-th/9508135; P. Di Vecchia, A. Lerda, L. Magnea and R. Marotta, Phys. Lett. B351:445 (1995), hep-th/9502156; P. Di Vecchia, A. Lerda, L. Magnea, R. Marotta, and R. Russo, preprint hep-th/9601143.
- [56] N.I. Usyukina and A.I. Davydychev, Phys. Lett. 298B:363 (1993); 305B:136 (1993); B332:159 (1994); B348:503 (1995); D. Kreimer, Phys. Lett. B347:107 (1995), hep-ph/9407234; Mod. Phys. Lett. A9:1105 (1994); A.I. Davydychev and J.B. Tausk, preprint hep-ph/9504431.